

The Distributional Consequences of Climate Change: The Role of Housing Wealth, Expectations, and Uncertainty

[[Click here for latest version](#)]

Jeffrey E. Sun

October 30, 2023

Abstract

In the United States, the majority of the median household's wealth is in the form of a single climate-exposed asset: their home. I study how this shapes inequality in welfare losses from climate change. In reality, house prices are location-specific, forward-looking, and determined in equilibrium by households uncertain about the future. I build a dynamic spatial equilibrium model of the U.S. with 1713 locations, incorporating heterogeneous and forward-looking households whose housing wealth depends on prices which they endogenously determine in spatially-segmented housing markets subject to climate news shocks and migration responses. I find the otherwise-intractable global solution under climate uncertainty using a novel but simple and general deep learning method. I quantify the model using harmonized recent estimates of climate impacts on local productivity, amenities, maintenance costs, and disaster risk. I discipline uncertainty using climate projections and time series data on homeowners insurance premiums. Inequality in climate damages is large, though initially progressive by wealth. However, climate uncertainty causes ongoing regressive wealth transfers as higher housing asset risk is passed on to poorer households through higher rents. Incorporating homeownership reverses the ameliorative effects of migration adaptation for spatial inequality in welfare losses from climate change. With housing wealth, a switch from widespread climate denial to widespread climate acceptance causes a transfer of almost \$1tn of housing wealth from households in more-harmed to less-harmed regions.

1 Introduction

In the United States, housing wealth accounts for approximately one third of household wealth¹, or \$51.9 trillion (Zillow). The value of every individual home within this stock depends on current expectations about the economic future of its location: a future that will be shaped by climate change.

I study how homeownership—ownership by households of these climate-sensitive housing assets—shapes inequality in welfare losses from climate change. Complexity arises from the fact that the effects of climate change on housing wealth go through forward-looking equilibrium housing prices. Climate change, climate news, and climate uncertainty all create demand responses which nonlinearly determine housing prices and rents in spatial and intertemporal equilibrium. Even the first order effects of physical climate change on

¹Q2 2023 household net worth (FRB), \$154.3tn.

demand are complex, as the impacts of global climate change are heterogeneous across space and affect multiple factors of housing and location choice, even within locations. A final consideration is that the ownership of housing wealth is endogenous, so that current expectations shape not only current housing prices, but also who is exposed to future price changes.

To quantify the role of housing wealth in shaping inequality in welfare losses from climate change, I split the problem into four parts. First, I quantify climate damages to economic fundamentals: how global climate conditions affect economic fundamentals driving housing and location choice. Second, I quantify expectations and uncertainty over future global climate conditions. Third, I build a model to understand the response of equilibrium housing prices and housing asset ownership to climate changes, news, and uncertainty. Fourth, I solve this model under conditions of aggregate climate uncertainty. The global solution is made possible by a novel, but simple and general, deep learning method that I develop for solving recursive economic models with aggregate uncertainty.

Climate Damages to Economic Fundamentals—I combine and harmonize estimates from the literature to quantify the impact of global climate conditions on four specific local economic fundamentals: disaster risk, labor productivity, amenities,² and residential energy costs. The overall strategy is to combine projections from climate science on the impact of global climate conditions on local climate conditions with estimates from environmental economics on the impacts of local climate conditions on fundamentals. The primary challenge is avoiding double-counting: for each damage estimate I import, it is essential that the methodology used to generate it controls for the effects picked up by the other estimates. Additionally, estimates are reported in terms of different local climate variables. I show that, in the global temperature range of interest, both the climate science and environmental economics estimates are well-approximated³ by linear (or log-linear) functional forms, taking (1) global temperatures to local heating- and cooling-degree-days⁴ and (2) local heating- and cooling-degree-days to economic fundamentals. This allows the modeled sensitivities of local economic fundamentals to global climate conditions to be fully-flexibly location-specific while remaining functionally simple due to local (log-)linearization.

Expectations and Uncertainty—I combine climate and emissions projections with time series data on historical homeowners insurance premiums to quantify key parameters of climate expectations and uncertainty: the market-relevant distribution of possible future climate paths. Quantifying overall climate uncertainty is challenging because multiple sources of uncertainty contribute to overall uncertainty in qualitatively different ways. The Intergovernmental Panel on Climate Change (IPCC) defines three major sources of global climate uncertainty: internal variability (natural fluctuations in climate conditions), scenario uncertainty (uncertainty over the path of future emissions), and model uncertainty (uncertainty over the climate im-

²A location-specific quality-of-life shifter.

³For disaster damages, data limitations preclude this check.

⁴Heating- and cooling-degree-days are a measure of how cold and hot a location is, respectively, relative to 18.3°C (65°F). See Section 3.2 for a formal definition.

pacts of emissions).⁵

To calibrate overall climate uncertainty, I map data on each source of uncertainty to an interpretable auxiliary model of climate expectations, then match the climate process in the full model to the key moments of the auxiliary model. The auxiliary model consists of stochastic emissions and climate processes and a Bayesian household which can observe realized climate outcomes but has imperfect information about the parameters of the generating process. I quantify internal variability—natural climate variation from year to year—using historical data on annual temperatures from the National Centers for Environmental Information (NCEI) and historical data on disaster damages from the Spatial Hazard Events and Losses Database for the United States (SHELDUS). I quantify scenario uncertainty in the future path of emissions by setting the quartiles of 2020-2100 emissions to the values given by IPCC emissions scenarios RCP2.6, RCP4.5, and RCP6.0.

I quantify model uncertainty for temperatures and disaster risk separately. I calibrate model uncertainty over the contribution of emissions to temperatures using the variance of the estimates in the Coupled Model Intercomparison Project 5 (CMIP5) ensemble (Rasmussen & Kopp, 2017). I quantify model uncertainty in the contribution of emissions to disaster damages using historical data on the responsiveness of homeowners insurance premiums to disaster realizations and emissions. Empirically, homeowners insurance premiums rise in response to costly disasters, suggesting that markets' beliefs about disaster frequencies are uncertain enough to be affected by such realizations. I estimate this uncertainty using a Bayesian state space model.

Housing Price Responses, Household Wealth Exposures, and Welfare—In order to understand how climate change, climate news, and climate uncertainty affect individual households heterogeneously, I add individual housing ownership to a dynamic spatial equilibrium model of the contiguous U.S. with 1713 locations. The primary challenges are (1) incorporating the determinants of local housing prices and their response to climate change, news, and uncertainty; (2) incorporating the determinants of household housing asset ownership; and (3) numerically solving the model under aggregate uncertainty. These challenges likely motivate some common simplifying assumptions in the dynamic spatial literature generally, such as the assumption that households all rent housing from absentee landlords. I endogenize housing prices by explicitly modeling heterogeneous households whose forward-looking consumption-savings, migration, and real estate investment decisions determine aggregate housing demand. Local housing prices arise through the intersection, in spatial and intertemporal equilibrium, of housing demand with durable housing stocks constructed according to spatially-heterogeneous local housing supply curves (as estimated by Saiz (2010)). In the dynamic equilibrium, uncertainty about future economic conditions shapes households' willingness to hold housing assets, which shapes housing prices, which shapes household wealth. Changes in expectations—either

⁵We might also expect considerable uncertainty over the economic model governing housing markets and equilibrium responses. This is beyond the scope of this study.

through durable changes to current climate conditions, news about future climate conditions, or changes in uncertainty about future climate conditions—affect household wealth in the present through housing values.

The household block of the model is modeled after Kaplan et al. (2020), although the household’s choice is over continuous housing quality as in Favilukis et al. (2017). This is embedded in a spatial equilibrium model with frictional migration and heterogeneous bilateral migration costs, similar to Borusyak et al. (2022). I calibrate the model to the 1713 locations⁶ covering the contiguous U.S. reported in the Public Use Microdata Sample (PUMS) of the 1990 U.S. Census. I estimate amenity values, housing supply cost shifters, and productivity shifters for each location, exactly matching empirical populations, housing prices, and mean wages. I calibrate the stationary steady state of the model to match key moments of the 1990-1992 U.S. economy, computed from the PUMS microdata and the 1992 Survey of Consumer Finances (SCF). I choose this relatively early year for my primary calibration to allow for the role of anticipatory adjustment in shaping current populations, housing stocks, and asset holdings.

Numerical Solution—With aggregate climate uncertainty, this is a high state space model. The household’s policy function is, in principle, a function of the entire distribution of household states. A global solution with conventional methods is infeasible. In order to capture realistic changes in housing wealth, however, it is important to incorporate the effect, on housing prices and rents, of the existence and slow resolution of aggregate climate uncertainty. And because climate scenarios differ substantially and impact housing prices in complex, nonlinear ways, it is important to compute the global solution rather than use local approximations. In order to solve the model, I develop a novel, but simple and general deep learning method capable of solving dynamic spatial models with forward-looking heterogeneous agents facing complex frictions and aggregate uncertainty. In particular, I exploit the fact that, if a model is solvable in steady state, then it is generally the case that the household’s decision can be derived from current prices and the conditional continuation values⁷ faced by the household. (For instance, I use a simple grid-based method.) If this is the case, then it suffices to use a neural network to approximate: (1) the expected continuation value as a function of individual and aggregate state, (2) price functions as a function of the aggregate state. I take the concept of using a neural network to approximate the price function from Azinovic et al. (2022), and the method for optimally reducing the dimension of the aggregate state from Han et al. (2021). Unlike these papers, however, this method does not use a neural network to approximate the policy function. This removes common restrictions on the types of models which can be solved by deep learning methods, for instance that the value function be quasiconvex and differentiable in the policy variable.

This paper connects to a number of literatures.

First, a growing dynamic spatial environmental economics literature seeks to understand heterogeneity

⁶Public Use Microdata Areas (PUMAs)

⁷i.e. $\mathbb{E}[x | \Gamma]$, for some end-of-period individual state x and aggregate state Γ .

in the welfare impacts of climate change, typically focusing on between-location heterogeneity. A key theme in this emerging literature is understanding how spatial climate damages are shaped by (1) different climate impacts and (2) different adaptation mechanisms. A seminal paper without dynamics, Hsiang et al. (2017) consider spatial climate impacts on disasters, mortality, productivity, energy costs, and crime, but do not incorporate economic or migration adaptation. Desmet et al. (2021) study the impact of land loss due to coastal flooding and find that adaptation through the dynamic responses of investment and migration largely ameliorate losses to global GDP. Krusell and Smith (2022) consider productivity impacts due to temperature and adjustment via capital mobility but not migration, finding that capital mobility does not significantly change results. Bilal and Rossi-Hansberg (2023) study the impact of disasters on capital depreciation. They introduce forward-looking migration in anticipation of climate change, finding that migration substantially reduces spatial inequality in climate damages.

In this tradition, I consider spatial climate impacts on disasters, productivity, energy costs, and amenities. I incorporate migration and anticipation and introduce individual housing wealth and the endogenous response of housing prices to climate change, news, and uncertainty. With housing wealth, migration does not ameliorate spatial inequality in climate damages, because the loss of economic activity in climate-exposed regions is capitalized into housing wealth losses for households in those regions. I also introduce within-location household heterogeneity and find that within-location heterogeneity in climate welfare impacts by wealth, income, housing wealth, and age are approximately twice as large as between-location heterogeneity. Additionally, I introduce uncertainty in household climate expectations and find that this uncertainty is largely capitalized into higher rents and lower housing prices, effectively shifting the costs of climate risk from wealthier landlords to poorer renters. Among owners of real estate, wealthier households with endogenously lower absolute risk aversion benefit from climate uncertainty through increased risk premia on housing assets. This, for them, more than counteracts the welfare costs of housing asset risk.

Second, a literature on flood policy studies the role of government in subsidizing flood insurance and investing in flooding mitigation. These include Balboni (2021), Hsiao (2023), and Pang and Sun (2023). Fried (2022) incorporates household homeownership in a dynamic model with two locations.

Third, a new dynamic spatial literature seeks to understand how forward-looking agents make frictional decisions and/or respond to shocks in spatial equilibrium. These include Crews (2023), Komissarova (2022), and Kleinman et al. (2023). A subset of these papers specifically incorporate housing wealth, such as Giannone et al. (2023), Greaney (2021), and Fried (2022).

I draw from this literature methodologically and contribute to it by introducing fully local real estate and rental markets, uncertainty in the form of a stochastic transition, and a solution method for finding the global solution under aggregate uncertainty.

Fourth, an emerging literature develops tools to use deep learning to solve dynamic models with aggregate

uncertainty, which in turn can be connected to the literature spawned by Krusell and Smith (1998) on the solution of dynamic models with aggregate uncertainty through state space reduction. This literature includes Azinovic et al. (2022), Han et al. (2021), Maliar et al. (2021), and Fernandez-Villaverde et al. (2020).

Fifth, I draw from a housing literature which provides the foundation for understanding and modeling the household's housing and homeownership choice, either alone or in equilibrium. These include Sinai and Souleles (2005), Kaplan et al. (2020), and Favilukis et al. (2017). Yao and Zhang (2005) specifically study the relationship between wealth, portfolio choice, and asset returns.

The paper is structured as follows. In Section 2, I describe a dynamic spatial equilibrium model relating climate conditions and expectations to local housing prices, migration, and housing asset ownership. In Sections 3, 4, and 5, I quantify the model. In Section 3, I quantify the impact of global climate conditions on local economic fundamentals (amenities, labor productivity, energy costs, and disaster risk) by combining and harmonizing estimates from the climate science and environmental economics literatures. In Section 4, I quantify expectations and uncertainty over the future course of climate change using the full distribution of CMIP5 projection ensembles and time series data on historical homeowners insurance premiums. In Section 5, I calibrate the economic model to match spatial and aggregate U.S. data from the 1990 Census and 1992 SCF. In Section 6, I explore how housing ownership and uncertainty shape inequality in welfare losses from climate change in the calibrated model, both within and between locations. Section 7 concludes.

2 A Dynamic Spatial Equilibrium Model

2.1 Overview

I describe an overlapping-generations, small open economy model with multiple locations and spatially-segmented housing rental and residential real estate markets.

Time is discrete. The economy is populated by a distribution of households who differ in their bond holdings, human capital, real estate holdings, and age, and make forward-looking location, saving, and real estate investment decisions, subject to a number of spatial and financial frictions.

Each period, each household selects a single location to live and work in, paying monetary and utility migration costs if they change locations. Bilateral utility migration costs vary by origin-destination location pair.

Households may save through a risk-free bond or by purchasing residential real estate. The bond is issued by an overseas entity and its interest rate is exogenous. When buying real estate, households may obtain a mortgage in the form of negative bondholdings, subject to a collateral constraint and a higher interest rate than on savings. In equilibrium, due to this illiquidity, risk, and borrowing constraint, residential real estate assets offer a higher expected return than the safe bond.

All housing in each location is owned and occupied by households living in that location, though the owner and the occupier need not be the same household. Instead, a household may own housing and let it out to other households in the same location, generating a stochastic cash flow. Households who do own their home benefit in the form of lower maintenance costs. However, real estate is exposed to climate risk and transaction costs.

Housing is durable and the housing stock depreciates over time. New housing is constructed by a static, competitive construction sector. In effect, the quantity of housing in each location is given by the cost curve if prices are sufficiently high, otherwise by the depreciated stock of existing housing.

Housing rent and real estate prices are determined in equilibrium in each location and period. By contrast, the labor and goods markets are stylized. Production functions are linear, though productivity differs by location. Households supply labor inelastically and are paid their marginal product in the form of the consumption good, a costlessly tradable numeraire. There is no capital.

Climate change introduces aggregate uncertainty. Locations have systematically heterogeneous exposure to aggregate climate conditions, as described in Section 3, affecting productivity, amenities, energy costs, and disaster risk. These climate damages affect location and portfolio choices, which in turn affect equilibrium housing prices.

Households are ex ante identical with constant relative risk aversion. However, absolute risk aversion varies endogenously, decreasing in consumption wealth. Climate uncertainty thus affects households heterogeneously by wealth and age.

The full set of frictions that households in the model are subject to are: uninsurable idiosyncratic income and real estate value risk, uninsurable aggregate climate risk, migration costs, real estate transaction costs, borrowing limits, and borrowing costs.

2.2 Households

At the beginning of each period, the economy is populated by a distribution of households $x \in \mathbf{X}$. Individual households, indexed by $i \in I$, are atomistic, with beginning-of-period state

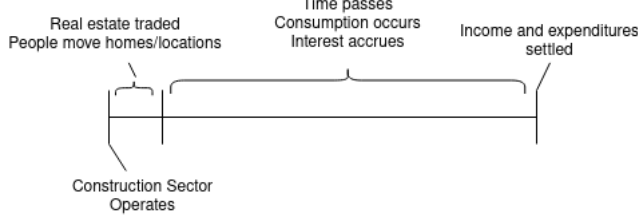
$$x_{it} = (b_{it}, z_{it}, h_{it-1}^{\text{live}}, h_{it-1}^{\text{let}}, \ell_{it-1}, a_{it}),$$

consisting of bondholdings b_{it} , human capital z_{it} , owner-occupied real estate h_{it-1}^{live} , owned rental real estate h_{it-1}^{let} , location ℓ_{it-1} , and age a_{it} . Owner-occupied real estate h_{it-1}^{live} , possibly zero, is owned by the household and was occupied by the household in the previous period. Rental real estate h_{it-1}^{let} , possibly zero, is owned by the household and was leased out to renters in the previous period. All housing variables are continuous and expressed in units of equal price.

2.2.1 Timing

Households live for a_{max} periods.⁸ Each period consists of two phases. First, an adjustment phase: households draw location preference shocks, trade housing assets and may move across space. Second, an immobile phase: households earn and consume, and settle flow income and expenditures at the end of the period.

Aggregate shocks are realized at the end of the period, after all households actions. A construction sector operates at the beginning of the period, before all household actions.



Each period, each household:

Adjustment Phase

- Inherits state $x_{it} = (b_{it}, z_{it}, h_{it-1}^{\text{live}}, h_{it-1}^{\text{let}}, \ell_{it-1}, a_{it})$
- Draws location preference shocks $\{\varepsilon_{\ell it}\}_{\ell}$.
- Observes real estate and rental prices $\{q_{\ell t}, \rho_{\ell t}\}_{\ell}$ in each location.
- Chooses location ℓ , real estate assets h_{it}^{live} and h_{it}^{let} , goods consumption g_{it} , and rental housing h_{it}^{rent} .
- Possibly adjusts their location ℓ and real estate assets $h_{it}^{\text{live}}, h_{it}^{\text{let}}$.

Immobile Phase

- Consumes goods and housing.
- Receives income: earnings, interest, and rent.
- Pays expenses: goods consumption, interest, rent, and maintenance.
- Realizes next-period human capital z_{it+1} .

Aggregate shocks are realized at the end of the period.

⁸In my calibration, I set a period equal to a decade, and model only adult households. There are six age groups. The first is 21-30, and the last is 71-80.

2.2.2 Adjustment Phase

At the beginning of period t , a household i in location ℓ_{it-1} draws preference shocks $\varepsilon_{\ell it}$ for each location ℓ ,

$$\varepsilon_{\ell it} \sim \text{Gumbel}(0, \psi^{-1}) \quad \text{i.i.d.}$$

then enters the adjustment phase with state

$$(b_{it}, z_{it}, h_{it-1}^{\text{live}}, h_{it-1}^{\text{let}}, \ell_{it-1}, a_{it}, \{\varepsilon_{\ell it}\}_\ell),$$

and chooses real estate, location, goods consumption, and rental housing $\{h_{it}^{\text{live}}, h_{it}^{\text{let}}, \ell_{it}, g_{it}, h_{it}^{\text{rent}}\}$. The household cannot occupy both a rented home and an owned one, so

$$h_{it}^{\text{live}} h_{it}^{\text{rent}} = 0.$$

2.2.3 Adjustment Frictions

The household is subject to: mobility costs, real estate transaction costs, borrowing costs, and a borrowing constraint. If they move to a new location, with

$$\ell \equiv \ell_{it}$$

$$\neq \ell_0 \equiv \ell_{it-1}$$

they pay a fixed monetary cost F^m and a utility cost depending on distance $d(\ell, \ell_0)$,

$$F^u(\ell, \ell_0) = \tau d(\ell, \ell_0).$$

If the household adjusts either type of real estate h_{it-1}^s , $s \in \{\text{live}, \text{let}\}$, they pay a percentage of the sale price $q_{\ell_0 it} h_{it-1}^s$ as a realtor's fee,

$$\phi q_{\ell_0 it} h_{it-1}^s.$$

Post-adjustment bondholdings may be negative, but the interest rate on borrowing r^m is higher than the interest rate on saving r^f ,

$$r^m > r^f.$$

After the adjustment phase, the household's wealth is

$$\tilde{b}_{it} = b_{it} - F^m D_{it}^{\text{move}} + \sum_{s \in \{\text{live}, \text{let}\}} D_{it}^{\text{sell}, s} [(1 - \phi) q_{\ell_0 t} h_{it-1}^s - q_{\ell t} h^s],$$

where $D^{\text{move}} = \mathbb{1}[\ell \neq \ell_0]$

$$D^{\text{sell}, s} = D^{\text{move}} \vee \mathbb{1}[h_{it-1}^s \neq h_{it}^s] \quad \forall s \in \{\text{live}, \text{let}\}.$$

2.2.4 Immobile Phase

The household enters the immobile phase with state

$$\tilde{x}_{it} = (\tilde{b}_{it}, z_{it}, h_{it}^{\text{live}}, h_{it}^{\text{let}}, \ell_{it}, a_{it})$$

with bondholdings \tilde{b}_{it} , human capital z_{it} , occupied real estate h_{it}^{live} , rental real estate h_{it}^{let} , and age a_{it} .

2.2.5 Consumption and Expenses

The household chooses⁹ numeraire goods consumption g_{it} . If $h_{it}^{\text{live}} > 0$, they occupy the owned housing,

$$h_{it} = h_{it}^{\text{live}}.$$

If $h_{it}^{\text{live}} = 0$, they choose and occupy rental housing,

$$h_{it} = h_{it}^{\text{rent}}.$$

If the household rents, they pay rent at rate $\rho_{\ell t}$. If they own real estate, they must pay maintenance at rate $\chi_{\ell t}^{\text{live}}$ or $\chi_{\ell t}^{\text{let}}$ for occupied or rented-out housing, respectively. Maintenance consists of a fixed cost depending only on whether the home is owner-occupied, and state- and location-dependent energy costs $y_{\ell t}$ and homeowner's insurance premium $\pi_{\ell t}$,

$$\begin{aligned} \chi_{\ell t}^{\text{live}} &= \chi^{\text{live}} + y_{\ell t} + \pi_{\ell t} \\ \chi_{\ell t}^{\text{let}} &= \chi^{\text{let}} + y_{\ell t} + \pi_{\ell t}, \\ \text{with } \chi^{\text{live}} &< \chi^{\text{let}}. \end{aligned}$$

⁹Consumption and rental housing are effectively chosen simultaneously with real estate and location, as no shocks occur between the adjustment and immobile phases, but in fact they only depend on \tilde{x}_{it} .

Total expenditures are,

$$\text{Expenditures}_{it} = \underbrace{g_{it}}_{\text{goods}} + \underbrace{\rho_{\ell t} h_{it}^{\text{rent}}}_{\text{rent}} + \underbrace{\chi_{\ell t}^{\text{live}} h_{it}^{\text{live}} + \chi_{\ell t}^{\text{let}} h_{it}^{\text{let}}}_{\text{maintenance}} + \underbrace{r^m b_{it} \mathbb{1}[b_{it} < 0]}_{\text{interest expenses}}.$$

2.2.6 Income

Given location-level productivity $A_{\ell t}$ and rent $\rho_{\ell t}$, the household receives labor earnings, interest income, and rental income,

$$\text{Income}_{it} = \underbrace{A_{\ell t} e^{z_{it}}}_{\text{earnings}} + \underbrace{r^f \tilde{b}_{it} \mathbb{1}[\tilde{b}_{it} \geq 0]}_{\text{interest income}} + \underbrace{\rho_{\ell t} h_{it}^{\text{let}}}_{\text{rental income}}.$$

2.2.7 Borrowing Constraint

Bondholdings at the end of the immobile phase are given by

$$b_{it+1} = R(\tilde{b}_{it}) + \underbrace{A_{\ell t} e^{z_{it}}}_{\text{earnings}} + \underbrace{\rho_{\ell t} h_{it}^{\text{let}}}_{\text{rental income}} - \underbrace{g_{it}}_{\text{goods}} - \underbrace{\rho_{\ell t} h_{it}^{\text{rent}}}_{\text{rent}} - \underbrace{\chi_{\ell t}^{\text{live}} h_{it}^{\text{live}} - \chi_{\ell t}^{\text{let}} h_{it}^{\text{let}}}_{\text{maintenance}}.$$

The household faces two borrowing frictions. First, a higher interest rate on borrowing than on savings,

$$R(b_{it}) = \begin{cases} (1 + r^f) b_{it} & b_{it} \geq 0 \\ (1 + r^m) b_{it} & b_{it} < 0. \end{cases}$$

Second, a collateral constraint or loan-to-value limit,

$$b_{it+1} \geq -\kappa q_{it\ell} (h^{\text{live}} + h^{\text{let}}).$$

2.2.8 Idiosyncratic Shocks

At the end of the immobile phase, the household's human capital evolves according to

$$z_{it+1} = p z_{it} + \zeta_{a_{it}} + \nu_{it}$$

$$\nu_{it} \sim \mathcal{N}(0, \sigma_\nu) \quad \text{i.i.d.},$$

where $p \in [0, 1]$ is mean reversion and ζ_a is an age-specific shifter.¹⁰

¹⁰This is isomorphic to the idiosyncratic human capital process of Kaplan et al. (2020), except that I pull out the aggregate productivity shifter $A_{\ell t}$ into the income equation.

Housing Asset Trade-Offs

The maintenance cost $\chi^{\text{let}} > \chi^{\text{live}}$ is higher for rental properties and captures the combination of: higher utility value of owner-occupied housing, higher maintenance and administrative requirements of a rental property, and income tax on rental income.

In equilibrium, homeownership is cheaper than renting for unconstrained households. Similarly, rental real estate provides higher expected returns than liquid assets. However, real estate comes at the cost of illiquidity and risk.

2.2.9 Utility

As in Kaplan et al. (2020), a household i in location ℓ derives utility from goods g_{it} , housing services h_{it} , and location-level amenities α_ℓ , with constant elasticity of substitution $1/\sigma$ between goods and housing services and constant elasticity of intertemporal substitution $1/\eta$. Location-level amenities enter as an effective multiplier on consumption spending. Formally,

$$u(g, h, \alpha_\ell) = \frac{\left(\alpha_\ell (g^{1-\sigma} + \gamma h^{1-\sigma})^{\frac{1}{1-\sigma}}\right)^{1-\eta} - 1}{1 - \eta}.$$

2.2.10 Full Household's Problem

In sum, the household's problem is given by

$$\begin{aligned}
& V_t(b, z, h_0^{\text{live}}, h_0^{\text{let}}, \ell_0, a, \{\varepsilon_l\}_l) \tag{1} \\
&= \max_{h^{\text{live}}, h^{\text{let}}, \ell, g, h} \varepsilon_l - \tau d(\ell, \ell_0) + u(g, h, \alpha_{\ell t}) + \beta \mathbb{E} V_{t+1}(b', z', h^{\text{live}'}, h^{\text{let}'}, \ell, a+1, \{\varepsilon'_l\}_l) \\
\text{s.t. } & u(g, h, \alpha_{\ell t}) = \alpha_\ell \frac{(g^{1-\sigma} + \gamma h^{1-\sigma})^{\frac{1-\eta}{1-\sigma}} - 1}{1-\eta} \\
& b' = R(\tilde{b}) + A_{\ell t} e^z + \rho_{\ell t} h^{\text{let}} - g - \rho_{\ell t} h^{\text{rent}} - \chi_{\ell t}^{\text{live}} h^{\text{live}} - \chi_{\ell t}^{\text{let}} h^{\text{let}} \\
& \tilde{b} = b - F^m D^{\text{move}} + \sum_{s \in \{\text{live, let}\}} D^{\text{sell}, s} [(1-\phi) q_{\ell_0 t} h_0^s - q_{\ell t} h^s] \\
& R(\tilde{b}) = \begin{cases} (1+r^f) \tilde{b} & \tilde{b} \geq 0 \\ (1+r^m) \tilde{b} & \tilde{b} < 0 \end{cases} \\
& b' \geq -\kappa q_{\ell t} (h^{\text{live}} + h^{\text{let}}) \\
& h = \begin{cases} h^{\text{live}} & h^{\text{live}} > 0 \\ h^{\text{rent}} & \text{otherwise} \end{cases} \\
& D^{\text{move}} = \mathbb{1}[\ell \neq \ell_0] \\
& D^{\text{sell}, s} = D^{\text{move}} \vee \mathbb{1}[h_0^s \neq h^s] \quad \forall s \in \{\text{live, let}\}
\end{aligned}$$

Expected continuation utility is defined as

$$\mathbb{E} V_{t+1}(b', z', h^{\text{live}'}, h^{\text{let}'}, \ell, a+1) \equiv \mathbb{E}_{z', h^{\text{live}'}, h^{\text{let}'}, \{\varepsilon'_l\}_l} [V_{t+1}(b', z', h^{\text{live}'}, h^{\text{let}'}, \ell, a+1, \{\varepsilon'_l\}_l) \mid z, h^{\text{live}}, h^{\text{let}}]$$

with stochastic transitions,

$$\begin{aligned}
\text{s.t. } & z_{it+1} = p z_{it} + \zeta_{a_{it}} + \nu_{it} \tag{2} \\
& \nu \sim \mathcal{N}(0, \sigma_\nu) \\
& \delta_{it}^{\text{live}}, \delta_{it}^{\text{let}} \sim \text{Beta}(\alpha_\delta, \beta_\delta) \\
& \varepsilon_{\ell it} \sim \text{Gumbel}(0, 1)
\end{aligned}$$

After age $a = a_{\max}$, the continuation value is given by a bequest motive, and all real estate is sold,

$$\begin{aligned}
& V_{a_{\max}+1, t}(b, z, h^{\text{live}}, h^{\text{let}}, \ell) = Q \frac{\tilde{b}^{1-\eta}}{1-\eta} \\
\text{s.t. } & \tilde{b} = b + (1-\phi) (q_{\ell t} h^{\text{live}} + q_{\ell t} h^{\text{let}}).
\end{aligned}$$

The properties of the Gumbel distribution imply that households choose locations in proportion to the (exponentiated) value of living in that location (see Appendix D).

2.2.11 Household Distribution Transition Function

The individual policy function solving (1) maps beginning-of-period state $x \in \mathbf{X}$ to chosen end-of-period (pre-shock) state $x^{\text{choice}} \in \mathbf{X}^{\text{choice}}$,

$$\begin{aligned}\text{Policy}_t(x, \{\varepsilon_\ell\}_\ell) &= x^{\text{choice}} \in \mathbf{X}^{\text{choice}} \\ x^{\text{choice}} &= (b', z, h^{\text{live}}, h^{\text{let}}, \ell, a).\end{aligned}$$

For $\mathbf{X}_0^{\text{choice}} \subseteq \mathbf{X}^{\text{choice}}$, taking $\{\varepsilon_\ell\}_\ell$ as unknown, the structure of the Gumbel distribution gives,

$$\Pr_\varepsilon(\ell | b, z, h^{\text{live}}, h^{\text{let}}, \ell_0, a + 1; \Gamma_t) = \frac{\exp\left(\psi \tilde{V}_\ell(b, z, h_0^{\text{live}}, h_0^{\text{let}}, \ell_0, a)\right)}{\sum_l \exp\left(\psi \tilde{V}_l(b, z, h_0^{\text{live}}, h_0^{\text{let}}, \ell_0, a)\right)}$$

where

$$\tilde{V}(b, z, h_0^{\text{live}}, h_0^{\text{let}}, \ell_0, a) = \max_{h^{\text{live}}, h^{\text{let}}, g, h} \tau d(l, \ell_0) + u(g, h, \alpha_{\ell t}) + \beta \mathbb{E} V_{t+1}(b', z', h^{\text{live}'}, h^{\text{let}'}, l, a + 1, \{\varepsilon'_l\}_l),$$

subject to the same constraints as in (1). This naturally defines idiosyncratic and distributional transition functions from \mathbf{X} to $\mathbf{X}^{\text{choice}}$. For $\mathbf{X}_0^{\text{choice}} \subseteq \mathbf{X}^{\text{choice}}$,

$$\begin{aligned}P_t(\mathbf{X}_0^{\text{choice}} | x) &= \Pr_\varepsilon(\text{Policy}_t(x, \{\varepsilon_\ell\}_\ell) \in \mathbf{X}_0^{\text{choice}}) \\ \lambda_t^{\text{choice}}(\mathbf{X}_0^{\text{choice}}) &= \int_{x \in \mathbf{X}} P_t(\mathbf{X}_0^{\text{choice}} | x) d\lambda_t(x).\end{aligned}$$

The idiosyncratic transition function (2) defines idiosyncratic and distributional transition functions from $\mathbf{X}^{\text{choice}}$ to \mathbf{X} . For $\mathbf{X}'_0 \subseteq \mathbf{X}$,

$$\begin{aligned}T_t(\mathbf{X}'_0 | x^{\text{choice}}) &= \Pr(x' \in \mathbf{X}'_0 | x^{\text{choice}}) \\ \lambda_{t+1}(\mathbf{X}'_0) &= \int_{x \in \mathbf{X}} T_t(\mathbf{X}'_0 | x^{\text{choice}}) d\lambda_t^{\text{choice}}(x).\end{aligned}$$

2.2.12 Household Entry

The youngest age group, representing age 20, enter with state

$$x_{it} = (b_{it}, z_{it}, 0, 0, \ell_{it-1}, 1, \{\varepsilon_{\ell it}\}_\ell),$$

where $h_{it-1}^{\text{live}} = h_{it-1}^{\text{let}} = 0$ and $a_{it} = 1$. Bondholdings b_{it} and human capital z_{it} are drawn from an initial distribution

$$(b_{it}, z_{it} \mid a_{it} = 1) \sim \Lambda^{\text{init}}.$$

Initial location ℓ_{it-1} is equal to the population distribution of households in the fourth age group, representing age 50:

$$\Pr_t(\ell_{it} \mid a_{it} = 1) \sim \int_{x \in \mathbf{X}} \mathbb{1}[(\ell(x), a(x)) = (\ell, 4)] d\lambda_t(x).$$

2.3 Housing

At each time t , the stock of housing $H_{\ell t} \in \mathbb{R}^+$ in each location ℓ is a state variable. Housing is expressed in units of equal price, as in Fafilukis et al. (2017), which can be costlessly divided and linearly transformed into houses of any quality level $h > 0$.

Housing assets are traded in local residential real estate markets and rented in local housing rental markets. Markets are spatially segmented and all housing must be owned by households in the same location. A household may only own or rent housing in the location in which they live.

Housing depreciates over time and new housing is constructed by a static, competitive construction sector which produces with zero profit using a location-specific housing production function. Effectively, if prices in a location ℓ are sufficiently high, the housing stock $H_{\ell t}$ is given by the location-specific production cost curve, and if prices are low, the housing stock is given by the depreciated stock of existing housing, $\tilde{H}_{\ell t} \equiv (1 - \delta^h)H_{\ell t-1}$.

2.3.1 Residential Real Estate Market

Demand In any location ℓ and time t , during the immobile phase, the stock of housing $H_{\ell t}$ is entirely owned by households who live in that location. Denote demand for residential real estate by

$$H_{\ell t}^D = \int_{x^{\text{choice}} \in \mathbf{X}^{\text{choice}}} (h^{\text{live}}(x) + h^{\text{let}}(x)) \mathbb{1}[\ell(x) = \ell] d\lambda_t^{\text{choice}}(x^{\text{choice}}).$$

Supply The stock of housing carried over from period $t - 1$ to period t in location ℓ is

$$\tilde{H}_{\ell t} = \int_{x \in \mathbf{X}} (h_0^{\text{live}}(x) + h_0^{\text{let}}(x)) \mathbb{1}[\ell(x) = \ell] d\lambda_t(x) = (1 - \delta^h) H_{\ell t-1}.$$

Before real estate is traded, a competitive construction sector constructs a quantity $(H_{\ell t} - \tilde{H}_{\ell t})$ of new housing and then sells it onto the market. Their decision is static. The per-quality-unit cost of construction for each location is a location-specific convex function of the new level of housing $H_{\ell t}$, as in Greaney (2021) and Saiz (2010).

$$c_\ell(H) = \Pi_\ell H^{\beta_\ell}.$$

I assume that the construction sector is competitive, so that if $H_{\ell t} > \tilde{H}_{\ell t}$, then $q_{\ell t} = c_\ell(H_{\ell t})$. Housing supply is thus given by

$$H_{\ell t}^S(q) = \begin{cases} c_\ell^{-1}(q) & q \geq c_\ell(\tilde{H}_{\ell t}) \\ \tilde{H}_{\ell t} & q \in (0, c_\ell(\tilde{H}_{\ell t})) \\ H_{\ell t}^D(0) & q = 0 \end{cases} \quad (3)$$

where $H_{\ell t}^D(q)$ denotes housing demand given prices $q_{\ell t} = q$. If $q = 0$, then some housing may remain unpurchased, in which case it is destroyed and $H_{\ell t} < \tilde{H}_{\ell t}$.

Residential real estate markets are segmented by location. The equilibrium condition for each residential real estate market is

$$H_{\ell t}^S = H_{\ell t}^D. \quad (4)$$

2.3.2 Housing Rental Market

In each location ℓ , demand for rental housing is given by

$$H_{\ell t}^{\text{rent}} = \int_{x^{\text{choice}} \in \mathbf{X}^{\text{choice}}} (h^{\text{rent}}(x)) \mathbb{1}[\ell(x) = \ell] d\lambda_t^{\text{choice}}(x^{\text{choice}})$$

and demand for rental real estate is given by

$$H_{\ell t}^{\text{let}} = \int_{x^{\text{choice}} \in \mathbf{X}^{\text{choice}}} (h^{\text{let}}(x)) \mathbb{1}[\ell(x) = \ell] d\lambda_t^{\text{choice}}(x^{\text{choice}}).$$

Rental housing markets are also segmented by location. The equilibrium condition for each rental housing market is

$$H_{\ell t}^{\text{rent}} = H_{\ell t}^{\text{let}}. \quad (5)$$

2.4 Climate

Locations are heterogeneously exposed to global climate conditions, affecting local productivity $A_{\ell t}$, amenities $\alpha_{\ell t}$, residential energy costs $y_{\ell t}$, and disaster damages $\delta_{\ell t}$. Global climate conditions evolve according to a simplified process (which is calibrated to match moments generated by a richer model of climate change and Bayesian climate expectations described in Section 4).

2.4.1 Productivity, Amenities, and Energy Costs

Productivity $A_{\ell t}$, amenities $\alpha_{\ell t}$, and residential energy costs $y_{\ell t}$ are fully flexible by location both in their level and in their response to global temperature SST_t . I linearize (or log-linearize) this relationship:

$$\log A_{\ell t} = \log \bar{A}_{\ell} + A_{\ell}^g SST_t$$

$$\log \alpha_{\ell t} = \log \bar{\alpha}_{\ell} + \alpha_{\ell}^g SST_t$$

$$y_{\ell t} = \bar{y}_{\ell} + y_{\ell}^g SST_t$$

I argue in Section 3 that this linearization is reasonable around the $\sim 4^{\circ}\text{C}$ range of global temperatures of interest, for both the sensitivity of local temperatures to global temperatures and the sensitivity of these economic fundamentals to local temperatures.¹¹

In each location ℓ , disaster damages $\delta_{\ell t}^{\text{disaster}}$ per unit of housing are a constant multiple of the aggregate disaster intensity $\delta_t^{\text{disaster}}$ for that year:

$$\delta_{\ell t}^{\text{disaster}} = \delta_{\ell}^g \delta_t^{\text{disaster}}.$$

2.4.2 Global Climate State

The global climate state evolves according to the following stylized process. This is an approximant to the richer climate process which I take to the data, described in Section 4. The approximant process is calibrated to match key moments of the richer process but reduces the dimensionality of the climate shock from 5 to 1.

Each period t , the global climate state is given by

$$\mathbf{D}_t = \{w_t, m_t, \underbrace{SST_t}_{\text{Global Temperature}}, \underbrace{\delta_t^{\text{disaster}}}_{\text{Global Disaster Intensity}}\},$$

where w_t and m_t are state variables loosely corresponding to global energy generation and emissions efficiency¹², respectively, though their calibration in Section 4 adjusts them to account for scenario uncertainty

¹¹When local temperatures are measured in heating- and cooling-degree-days.

¹²or inverse emissions intensity

and model uncertainty.

An annual index of global anthropogenic climate forcing rates (loosely representing annual emissions) e_t is constructed as the product of a factor w_t that grows at constant rate and a factor m_t that grows faster than m_t , so that e_t starts near zero, grows once w_t becomes sufficiently large, then eventually trends to zero as m_t overtakes w_t . I am interested in the region of the process, away from the stationary distribution, where e_t is still positive. The evolution of m_t is stochastic, representing both uncertainty about future emissions and about the climate system's response to emissions. Formally,¹³

$$e_t = w_t m_t \tag{6}$$

$$\begin{aligned} \log w_{t+1} &= \log w_t + g^w \\ \log m_{t+1} &= \log m_t - \beta_m w_t + \varepsilon_t^m \\ \varepsilon_t^m &\sim \mathcal{N}(0, \sigma_m^2). \end{aligned}$$

Global temperature SST_t and disaster intensity δ_t (expressed as the deviation from pre-industrial levels¹⁴) follow an autoregressive process impacted by forcings e_t :

$$\begin{aligned} \text{SST}_{t+1} &= \rho_c \text{SST}_t + \beta_{\text{SST}} e_t \\ \log \delta_{t+1} &= \rho_\delta \log \delta_t + \beta_\delta e_t. \end{aligned}$$

Note that ε_t^m represents a persistent shock to the growth rate of temperatures and disaster damages. It represents a news shock about the future trajectory of climate change.

2.5 Recursive Stochastic Equilibrium

2.5.1 State Space

I now drop time t subscripts and define the evolution of the aggregate state in recursive form.

The beginning-of-period aggregate state Γ is,

$$\Gamma = (\lambda, \mathbf{H}, \mathbf{D}),$$

where $\lambda : \mathcal{P}(\mathbf{X}) \rightarrow \mathbb{R}$ is the measure over individual states $x \in \mathbf{X}$, $\mathbf{H} = \{\tilde{H}_\ell\}_\ell$ is the set of beginning-of-

¹³Note that this particular process does not admit simulation from the infinitely distant past because m_t is nonstationary. This is easily solved by substituting $\log m_{t+1} = \log m_t - (\rho_m + \varepsilon_t^m)w_t$, but this is unnecessary for the purposes of this study.

¹⁴Disaster damages at the pre-industrial baseline level can be considered a form of maintenance, whose spatial variation can be approximately soaked up by $\Pi_{\ell t}$.

period location-level housing stocks, and \mathbf{D} is the aggregate climate state. The model evolves according to the transition function

$$\Omega(\Gamma' | \Gamma).$$

2.5.2 Equilibrium

A recursive stochastic equilibrium is

- A set of household policy and value functions solving Equation (1),
- Aggregate transition functions over

$$\Gamma = \{\lambda, \mathbf{H}, \mathbf{D}\}$$

composed of transition functions over λ , \mathbf{H} , and \mathbf{D} defined by Equations (2), (3), and (6), respectively, and

- Prices $q_\ell(\Gamma)$, $\rho_\ell(\Gamma)$ satisfying the market clearing conditions in Equations (4) and (5), respectively.

2.6 Shock Concept

I consider an economy in an initial stationary steady state which unexpectedly begins to experience climate change. As soon as the climate process begins, households understand that it will continue following the process described in Section 2.4.2. To the extent that households collectively under- or overestimate climate change's severity, this will be reflected in the form of high or low draws of the climate news shock ε_t^m .

That is, the economy first experiences a single, unexpected shock bringing it from a stationary steady state to a “stochastic climate transition.” Each subsequent period, the economy experiences a climate news shock drawn from a known distribution.

Note that climate change is highly persistent but not permanent. Climate forcings e_t eventually trend to zero, after which temperature and disaster damage deviations-from-baseline also slowly regress to zero,

$$\lim_{t \rightarrow \infty} e_t = 0$$

$$\lim_{t \rightarrow \infty} \text{SST}_t = 0$$

$$\lim_{t \rightarrow \infty} \delta_t = 0,$$

returning the economy to the stationary steady state.

I use this stationary steady state as the initial aggregate state which experiences an unexpected climate transition. Specifically, I consider an initial stationary steady state in which $m_t = m = 0$. (The value of $w_t \in \mathbb{R}$ affects nothing.) After the shock, the values (m, w) are then unexpectedly set to (m_0, w_0) , which I

calibrate in Section 4. Note that all climate shocks, including this initial shock, do not affect current climate conditions, only expectations about future climate conditions.

To preview the calibration strategy described in detail in Section 5, I calibrate the initial stationary steady state to represent the United States in 1990-1992.¹⁵

3 Climate Damages

I spend the next three sections quantifying the model. In this section, Section 3, I combine and harmonize estimates from the climate science and environmental economics literatures to quantify the impact of global climate conditions on local economic fundamentals: productivity, amenities, energy costs, and disaster risks.

In Section 4, I calibrate the global climate process. I do this by constructing and quantifying a richer model of stochastic global climate change and Bayesian climate expectations, then calibrating the simpler climate process in the economic model to match key moments of the richer, quantified model.

In Section 5, I calibrate the remaining parameters of my economic model using data from the U.S. Census and Survey of Consumer Finances.

3.1 Global Climate Conditions → Local Economic Fundamentals

To calibrate the impact of global climate conditions on local economic fundamentals, I combine estimates of the impact of global climate conditions on local climate conditions with estimates of the impact of local climate conditions on local economic fundamentals:

Global Climate Conditions → Local Climate Conditions → Local Economic Fundamentals.

Available in the literature are estimates of local climate conditions under specific climate scenarios and estimates of the effects of local temperature metrics on local economic fundamentals. Furthermore, estimates of these local economic impacts may overlap in terms of the responses they measure.

To generalize estimates of local temperature responses to global climate conditions, I linearize between estimates for 2000 and 2080 under RCP4.5.

To combine and generalize estimates of the response of local economic fundamentals to local temperature metrics, I compile a set of studies whose methodologies, when applicable, each control for the effects measured by the other studies. Where available, I use nonparametric or overparameterized estimates and show that the effects measured are approximately linear in the temperature metric I choose. I therefore argue that I

¹⁵The fact that the far-future climate converges to its 1990 state, which is in reality around 0.6°C warmer than pre-industrial levels, has minimal impact on model predictions through 2100 century, since the climate process is calibrated to CMIP5 projections through 2100 anyway.

am able to linearize all the way through, obtaining reasonably linearized estimates of the responses of local economic fundamentals to global climate conditions.

Explicitly, I allow local labor productivity $A_{\ell t}$, amenities $\alpha_{\ell t}$, residential energy costs $y_{\ell t}$, and disaster damages to housing $\delta_{\ell t}$, to depend on global climate conditions. I allow these variables to be fully-flexibly location-specific in their levels and sensitivity to global climate conditions:¹⁶

$$\begin{aligned}\log A_{\ell t} &= \log \bar{A}_{\ell} + A_{\ell}^g \text{SST}_t \\ \log \alpha_{\ell t} &= \log \bar{\alpha}_{\ell} + \alpha_{\ell}^g \text{SST}_t \\ y_{\ell t} &= \bar{y}_{\ell} + y_{\ell}^g \text{SST}_t \\ \delta_{\ell t} &= \delta_{\ell}^g \bar{\delta}_t.\end{aligned}$$

I define $A_{\ell t}$ as a multiplier on the effective quantity of labor supplied by each household in a location. I define $\alpha_{\ell t}$ as a multiplier on the effective quantity of consumption enjoyed by each household in a location. I define $y_{\ell t}$ as the overall cost of energy required to heat and cool a typical owner-occupied two-bedroom in location ℓ over the course of period t . I define $\delta_{\ell t}$ as the average excess disaster damages due to climate change suffered by a typical owner-occupied two-bedroom housing unit in location ℓ in period t .

In Section 3.4, I report the general magnitudes and economic and spatial heterogeneity of these estimated climate damages, by I naively dollarizing and summing them for each household in the 2020 American Community Survey (ACS). By far the most severely affected individual counties are those exposed to severe flooding, primarily along the coast and in Central Appalachia. However, far more counties are exposed to temperature changes, such that overall damages due to temperature are larger than those due to flooding,

3.2 Global Climate Conditions → Local Climate Conditions

The relevant measures of local climate conditions that I use are heating degree days (HDD) and cooling degree days (CDD).

The number of heating (cooling) degree-days in a year is the number of degree-days in a year by which daily temperatures are below (above) 18.3°C (65°F). For location i , year t , days d ,

$$\begin{aligned}\text{HDD}_{i,t} &= \sum_{d \in D_t} \max(18.3 - T_{i,d,t}, 0) \\ \text{CDD}_{i,t} &= \sum_{d \in D_t} \max(T_{i,d,t} - 18.3, 0)\end{aligned}$$

I linearize between CMIP5 ensemble model median projections, under RCP8.5, of spatial HDDs and

¹⁶The intercept for $\delta_{\ell t}$ is zero because $\delta_{\ell t}$ and $\bar{\delta}_t$ are defined as the deviation from the same pre-industrial baseline.

CDDs, in 2000 and 2080. Figure 1 shows the projected change in HDD and CDD per °C global warming across space.

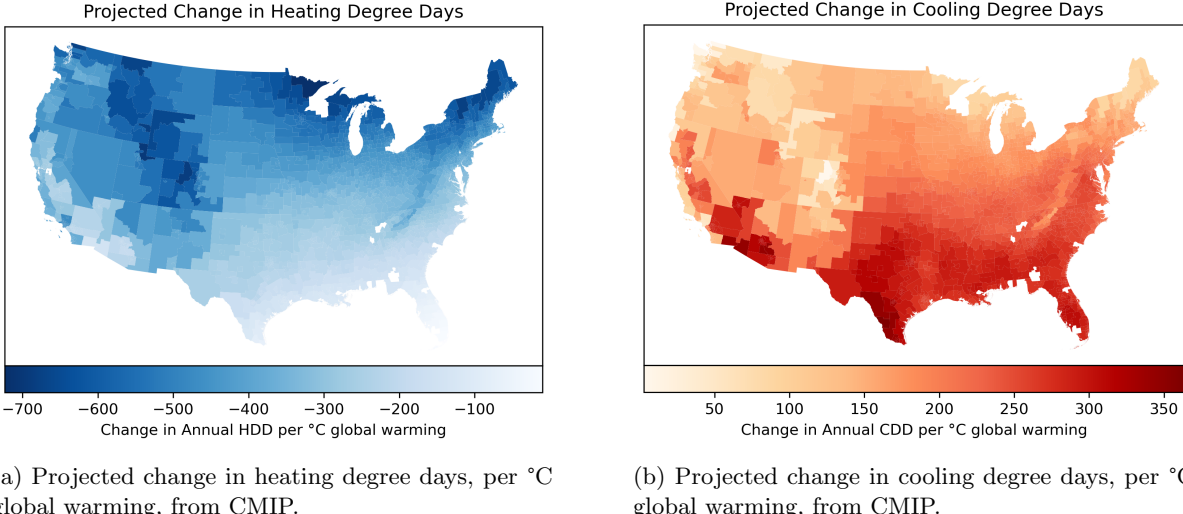


Figure 1

Projected change in heating and cooling degree days per °C global warming. I use CMIP5 (Gassert et al., 2021) estimates of projected HDD and CDD under RCP8.5 for 2000 and 2080. I assign to each PUMA the projected change in HDD and CDD at its centroid, and divide by the median projected warming under RCP8.5 (Hsiang et al., 2017) to obtain the change in HDD and CDD for each PUMA per °C global warming.

3.3 Local Climate Conditions → Local Economic Fundamentals

I now compile and harmonize estimates from the environmental economics literature on the impact of local climate conditions on local economic fundamentals: productivity, amenities, energy costs, and disaster risks. For each impact, I use estimates from a study which, when applicable, controls for each other impact in its methodology. This is necessary to prevent double-counting.

3.3.1 Labor Productivity

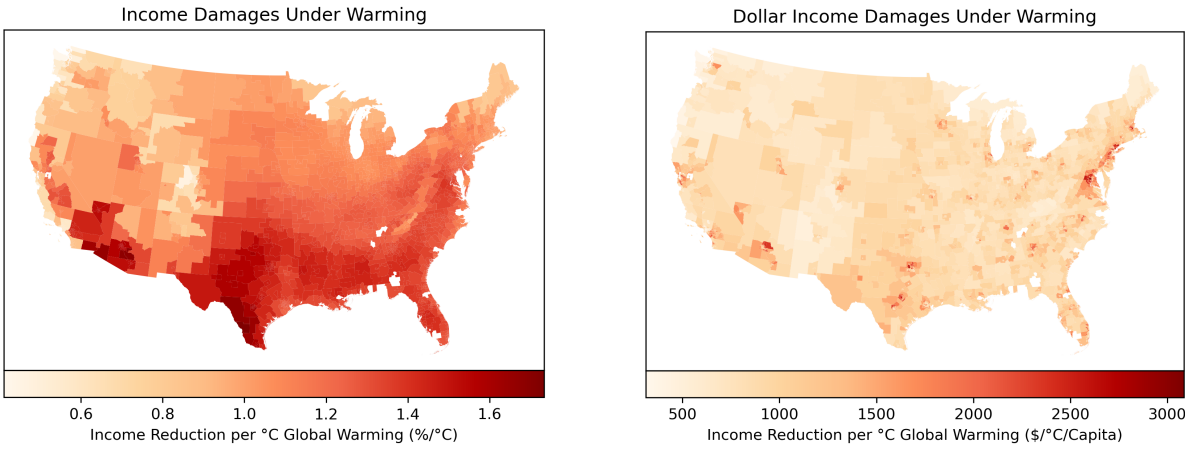
I take estimates of the effect of temperature on wages from Deryugina and Hsiang, 2017. They study the effect of weather variation on a panel of U.S. counties from 1969 to 2014 to estimate the effect of temperature on wages.¹⁷

¹⁷See Appendix Section A.1 for details.

Parameter	Productivity Effect per DD (%)	Productivity Effect per 365 DD (%)
HDD	6.57×10^{-6}	0.240
CDD	4.50×10^{-5}	1.66

Table 1: Productivity Damages per Heating and Cooling-Degree Day

Productivity damages per single ($^{\circ}\text{C}$) degree-day, and per 365 degree-days, relative to the 18.3°C (65°F) baseline, as a percentage of annual income. Column 2 represents the effect of 365 additional CDDs (HDDs), and represents the marginal damage (benefit) of a one-degree increase in temperature for each day of the year, in a location where every day is already above (below) 18.3°C .



(a) Percentage reduction in productivity per capita, per degree $^{\circ}\text{C}$ global warming. Estimates are from Deryugina and Hsiang, 2017. I linearize and multiply their estimates by the projected change in HDD and CDD per $^{\circ}\text{C}$ global warming, as described in Figure 1. Further details are in Appendix Section A.1.

(b) Naively dollarized reduction in productivity per capita, per degree $^{\circ}\text{C}$ warming. I merely multiply the percentage reduction in productivity as in Figure 2a by observed wages in the 2021 ACS.

Figure 2: Productivity Damages per $^{\circ}\text{C}$ Global Warming

3.3.2 Heat and Cold Disamenities

I take estimates of heat and cold disamenities from Albouy et al., 2016, expressed as a percentage of income. That is, they estimate the percentage of one's income one would be willing to give up in order to avoid a marginal day at a certain temperature. I believe that losing a percentage of one's income is a quantitatively similar cost to losing a percentage of one's consumption, which is how I introduce this damage into my model. Figure 3 shows the projected change in heat and cold disamenities, and 4 shows the projected net change.

Parameter	WTP per DD (% of Income)	WTP per 365 DD (% of Income)
HDD	3.05×10^{-3}	1.11
CDD	4.40×10^{-3}	1.61

Table 2: Amenity Damages per Heating- and Cooling-Degree Day

Column 1 represents willingness-to-pay to avoid a single ($^{\circ}\text{C}$) degree-day, relative the 65°F baseline, as a percentage of annual income. Column 2 represents the willingness to pay to avoid 365 CDD (HDD), and is equal to is Column 1 multiplied by 365. It represents the marginal damage (benefit) of a one-degree increase in temperature for each day of the year, in a location where every day is already above (below) 65°F .

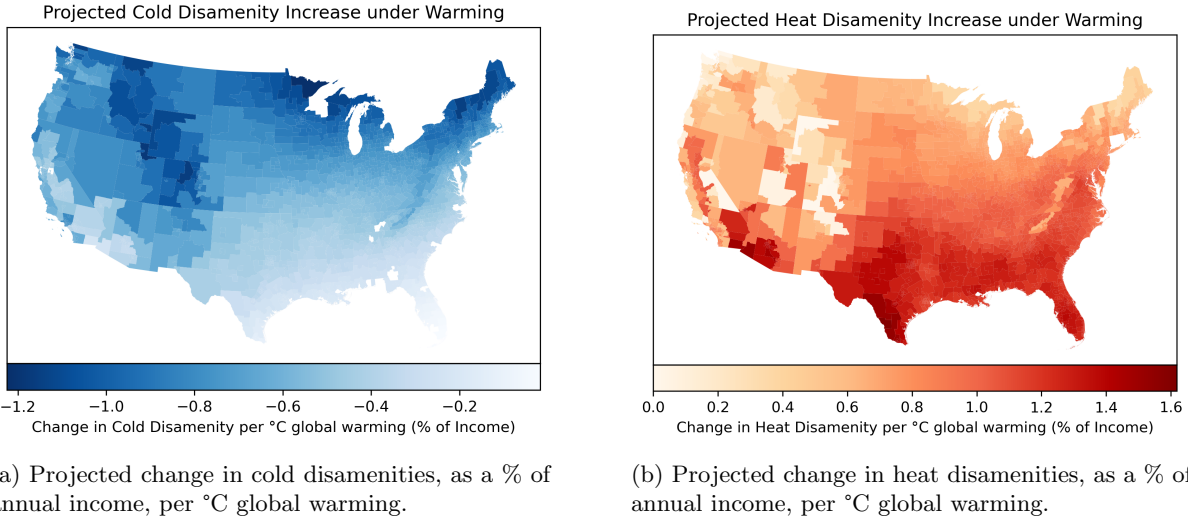


Figure 3: Heat and Cold Disamenities per $^{\circ}\text{C}$ Global Warming

Estimates of heat and cold disamenities from Albouy et al., 2016, expressed as a percentage of income. They use a Rosen-Roback style model to impute amenities for each U.S. PUMA as the residual of real wage differentials in the 2000 Census (5% sample). Their estimates are almost linear in HDD and CDD, so I linearize to obtain Table 2. I multiply these estimates by county-level HDD and CDD damage estimates. Disamenities generally increase in Southern latitudes and decrease in Northern.

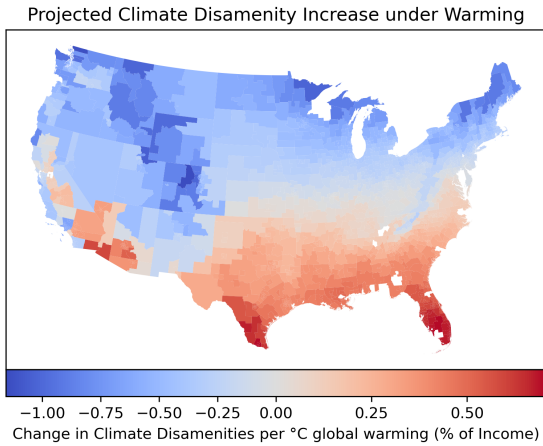
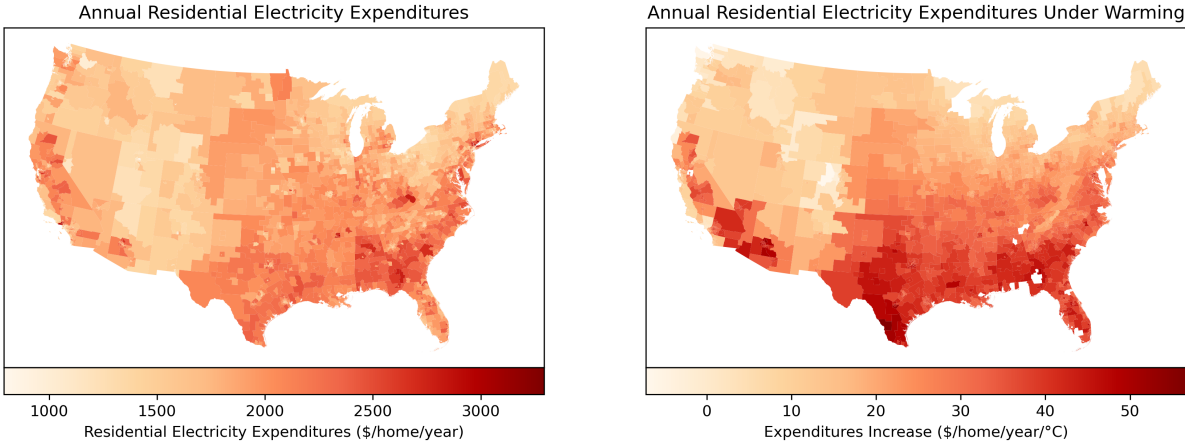


Figure 4: Net Climate Disamenities per °C Global Warming

Net projected change in cold and heat disamenities, as a % of annual income, per °C global warming. Estimates are obtained by separately computing heat and cold disamenities using estimates from Albouy et al., 2016 on disamenities per heating or cooling degree day (expressed as a percentage of income) and combining with estimates on the effect of global warming on local heating and cooling degree days from CMIP.

3.3.3 Energy Costs

I take projections of the effect of warming on energy costs from Rode et al., 2021. Figure 5a describes the current levels of residential electricity consumption per capita in the ACS. Figure 5b describes the projected change in energy expenditure per capita per °C global warming.



(a) Annual residential energy expenditure per capita, 2021. Data are from the 2021 ACS. The variable is directly reported, and aggregated using provided weights intended to be representative of local populations across the United States.

(b) Projected change in annual residential energy expenditure per capita (2021 USD), per $^{\circ}\text{C}$ global warming.

Figure 5: Residential Energy Expenditure Damages per $^{\circ}\text{C}$ Global Warming

Data are from the ACS and Rode et al., 2021. The latter project electricity consumption growth between 2020 and 2100 under RCP8.5 at the county level. To put these projections in per-degree- $^{\circ}\text{C}$ terms, I divide by the median projected global temperature increase between 2020 and 2100 under RCP8.5, which is 3.7°C . I multiply their projected percentage increase in total electricity consumption percentage by current levels of residential energy expenditure. They do not distinguish between residential and other energy consumption.

3.3.4 Disaster Damages

I use projections of climate impacts on total combined damages from flooding from Bates et al. (2021), as reported in Wing et al. (2022). The authors use a high-resolution inundation model to compute comprehensive coastal, fluvial, and pluvial flood risk, and are the first large-scale inundation model to incorporate all sources of flooding.

Flooding represents the large majority of projected climate damages through natural disasters. Figure 6 shows the relative property damages from flooding between 1975 and 2020 by FEMA hazard type. Damages which involve both storms and flooding are split evenly between the relevant flooding-related category and storm-related category. This may thus represent a significant underestimate of total damages from flooding, as flooding damages often occur in conjunction with storms. This leaves wind-related damages and wildfires as quantitatively large, plausibly climate-impacted hazards. However, recent climate literature projects only small (on average) and highly uncertain impacts of climate change on wind-related damages. Wildfires remain unaccounted for. I nevertheless conclude that using only flooding damages captures most disaster climate damages.¹⁸

Figure 7a displays their model-predicted AAL, as a percentage of residential structure value, under 2020

¹⁸See Appendix Section A.2 for details.

climate conditions. Figure 7b shows projected flooding damage growth, as a percentage of current AAL, per $^{\circ}\text{C}$ global warming. The largest value of the latter is 9.32%, indicating that an additional 9.32% of the entire housing structure value is lost each year per $^{\circ}\text{C}$ global warming.

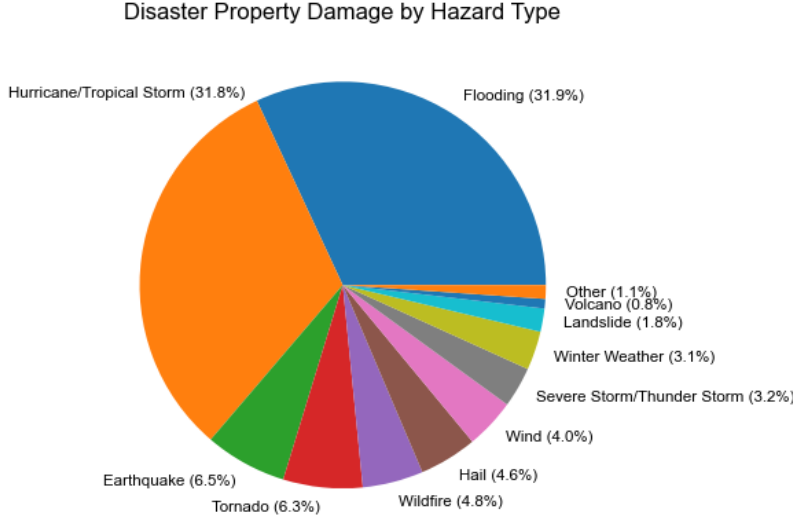
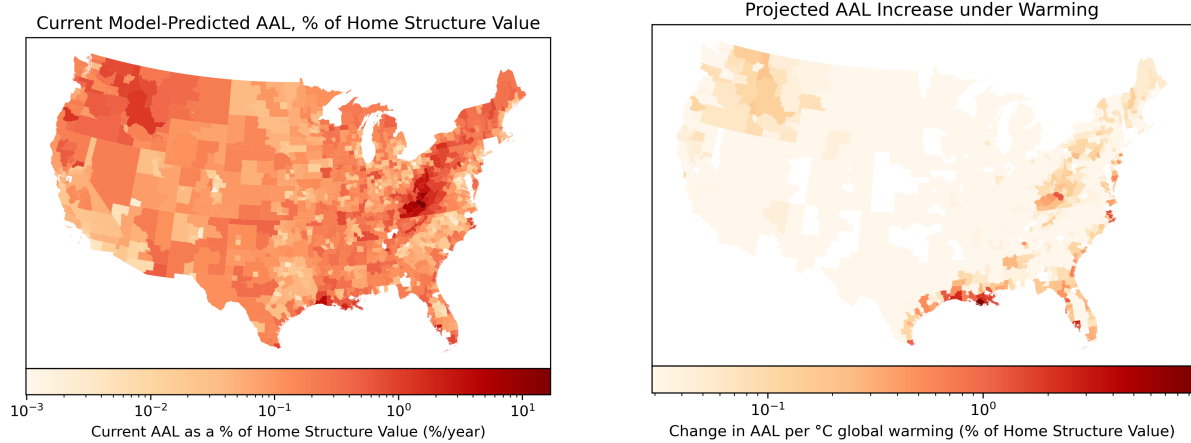


Figure 6: Total Disaster Property Damage by FEMA Hazard Type, Annual Mean 1975-2020. SHELDUS.



(a) Model-predicted annual residential flooding damages, Average Annual Losses (AAL), as a % of housing structure value. Source: Wing et al. (2022).

(b) Projected flooding damage growth as a percentage of housing structure value, log scale. Some values are negative: to create the plot I add 5 basis points to all values. Originally reported by Wing et al. (2022) as the percentage change in AAL, 2020-2050, under RCP 4.5. I multiply by estimates 20201 AAL, as Figure 7a, then divide by 0.63°C : the CMIP5 median temperature change, 2020-2050, under RCP 4.5.

Figure 7: Projected Flooding Damage Growth per $^{\circ}\text{C}$ Global Warming

3.4 Damage Magnitudes and Variation

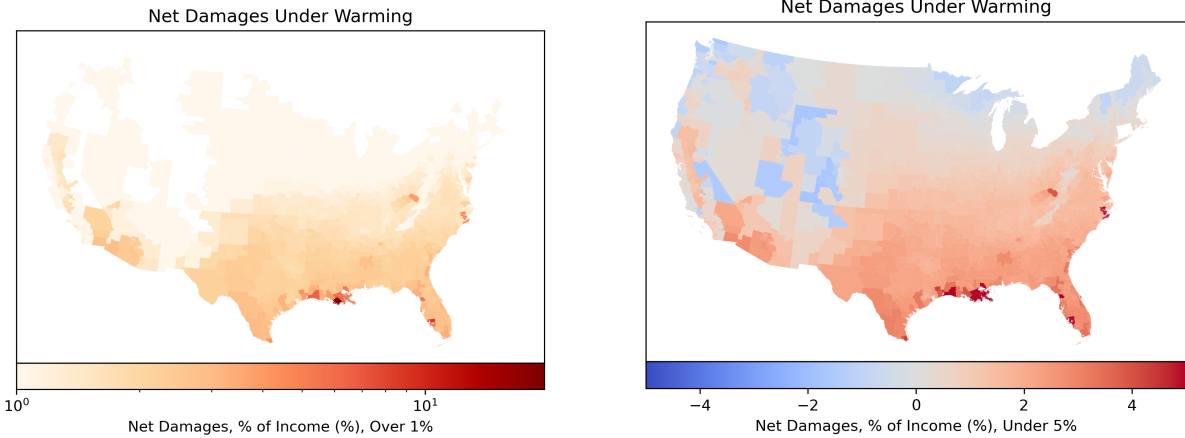
In order to understand the relative magnitudes and spatial distribution of these damages, I naively dollarize annual damages for every household in the ACS. Damages are per 1°C global warming. Damages are dollarized as follows. Productivity damages are multiplied by current income. Amenity damages are multiplied by current income. Residential energy expenditure damages are multiplied by current residential energy expenditures. Disaster damages are multiplied by current home structure values, if the home is owned, or set to zero if the home is rented.

The home structure value is imputed by multiplying the reported home value by FHFA county-level land share estimates.¹⁹ Figure 2 shows net damages from all sources combined. Figure 8a shows damages on a log scale to highlight the severity of damages in highly flooding-exposed counties. Figure 8b is on a linear scale to illustrate more widespread but less localized damages, mostly temperature-related.

Figure 9 compares damages, as a percentage of income, by income and by latitude. Damages are relatively flat by income partly by construction: productivity and amenity damages are constructed as a percentage of income. Nevertheless, flooding and energy cost damages are proportionally larger for lower-income households, due to housing price exposure and energy expenditure being larger for these households as a proportion of income.

Spatial inequality in damages is quite dramatic. Figure 9b shows damages by latitude. Households at lower latitudes experience significantly greater heat disamenities and productivity damages, and smaller decreases in cold disamenities. Flooding damages are relatively small as a proportion of total damages, but are highly spatially concentrated.

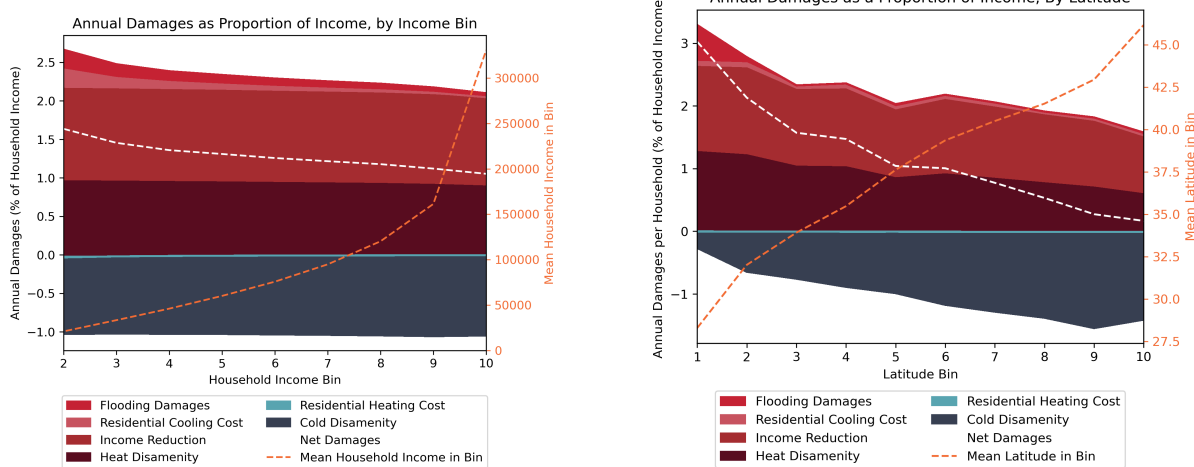
¹⁹I convert these to PUMAs using a population-based crosswalk. See Appendix E for the crosswalk procedure.



(a) Mean overall damages as a percentage of annual income, per $^{\circ}\text{C}$ global warming, aggregating over heating and cooling costs, heat and cold disamenities, income effects, and flooding damages. Bottom coded at 1%.

(b) Mean overall damages as a percentage of annual income, per $^{\circ}\text{C}$ global warming, aggregating over heating and cooling costs, heat and cold disamenities, income effects, and flooding damages. Top-coded at 3%.

Figure 8: Mean Overall Naively-Dollarized Damages by PUMA



(a) Damages, as a percentage of income, by income bin, per $^{\circ}\text{C}$ global warming. Estimates are obtained by harmonizing estimates for individual damages as described above, then imputing damages to each household in the 2020 ACS.

(b) Damages, as a percentage of income, by geographic latitude, per $^{\circ}\text{C}$ global warming. Estimates are obtained by harmonizing estimates for individual damages as described above, then imputing damages to each household in the 2020 ACS.

Figure 9: Economic vs. Spatial Inequality in Climate Damages

Figure 10 displays estimates along other spatial margins: distance to coast, latitude, and 2020 mean annual temperature. Damages are decreasing in distance from the coast. This is primarily driven by climate amenities and income impacts, through temperature, rather than flood risk, though flood risk is a contributor. Damages are strongly increasing in temperature, due largely to climate impacts on amenities and income, though flood risk is a contributor in this case too. Overall damages are positive for most counties, with

counties in the bottom temperature (mean annual temperature) decile still experiencing positive damages, and counties in the top temperature decile experiencing damages of almost 3% of income per °C global warming.

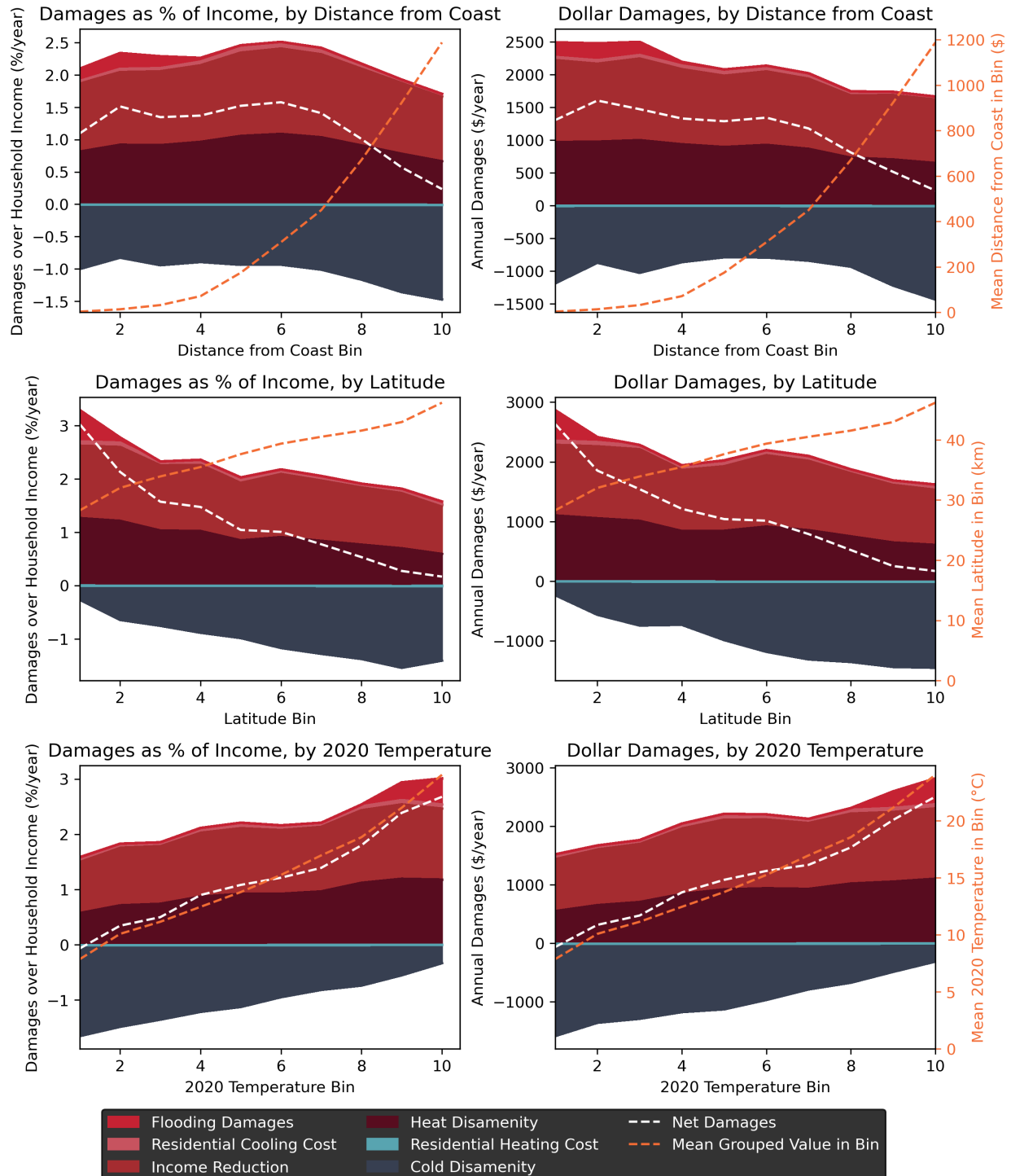


Figure 10: Individual damages by Income, Distance from Coast, and Urban Population Share of PUMA. Estimates are obtained by harmonizing estimates for individual damages as described above, then imputing damages to each household in the 2020 ACS.

4 Quantifying Climate Expectations

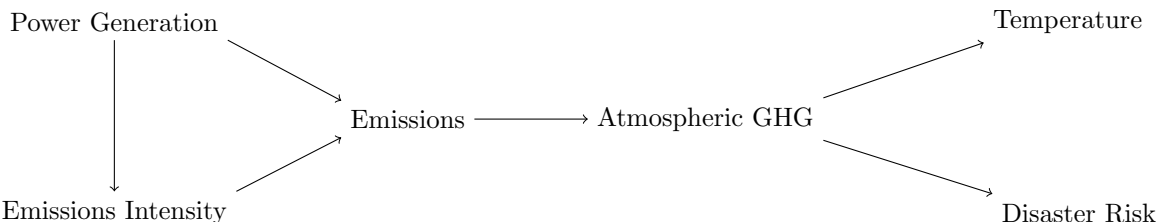
In this section I calibrate the climate process in the economic model using an auxiliary model. That is, I describe a model of climate expectations that is richer than the one-shock, full-information climate process in the economic model. The richer model is a model of a Bayesian agent learning about a stochastic climate process. The purpose of this auxiliary model is to explicitly incorporate multiple sources of climate variation and uncertainty, which can be quantified from the data. I then calibrate the simpler climate process in the economic model to match the key features of the auxiliary model. In particular, I match the quartiles of the Bayesian agent's prior, in 2020, over 2100 global temperatures and disaster damages.

I first describe a stochastic climate process. I then describe rational Bayesian learning for an agent who observes this process but does not know the sensitivities of temperature and disaster damages to emissions, instead having a Normal prior over these and observing temperature and disaster realizations and news shocks.

4.1 Stochastic Global Climate Process

I describe a process in which the evolution of global climate conditions is influenced by greenhouse gas (GHG) emissions. The purpose of this model is still not to be a realistic representation of the climate system, however. Instead, it is intended to parsimoniously encode, at any point, a plausible distribution of future climate paths, such that (1) news shocks affect the distribution of future paths in a plausible way, and (2) data on different sources of uncertainty can be mapped to the model in an interpretable way.

In this model, global power generation grows at a constant rate. The annual level of GHG emissions is the product of global power generation and the emissions intensity of power generation. The emissions intensity decreases over time, eventually overtaking power generation, so that emissions eventually vanish.²⁰ Emissions contribute to a stock of atmospheric GHGs which is gradually absorbed out of the atmosphere by natural processes. Annual mean temperatures and disaster damages are drawn each year from a distribution which depends on the stock of atmospheric GHG. This is illustrated below:



Formally, time is discrete. Global power generation w_t at time t is deterministic and grows at a constant

²⁰This process remains agnostic on the extent to which these emissions intensity reductions are due to policy responses or "natural" technological progress.

rate g^w :

$$\log w_{t+1} = \log w_t + g^w.$$

The emissions intensity of power generation, m_t , decreases in proportion to current power generation

$$\begin{aligned}\log m_{t+1} &= \log m_t - \beta_m w_t + \varepsilon_t^m \\ \varepsilon_t^m &\sim \mathcal{N}(\mu_m, \sigma_m).\end{aligned}$$

Annual emissions are simply the product of power generation and emissions intensity:

$$e_t = w_t m_t. \quad (7)$$

The stock of atmospheric greenhouse gases, GHG_t follows an autoregressive process. Anthropogenic emissions and natural sources contribute to it and it is naturally absorbed at rate ρ_{GHG} :

$$\text{GHG}_{t+1} = c_{\text{GHG}} + \rho_{\text{GHG}} \text{GHG}_t + e_t. \quad (8)$$

Annual temperatures are drawn from a distribution with mean $\overline{\text{SST}}_t$ which is linear in the stock of atmospheric GHG:

$$\overline{\text{SST}}_t = \tilde{c}_{\text{SST}} + \tilde{\beta}_{\text{SST}} \text{GHG}_t.$$

Substituting in Equations 7 and 8 and simplifying:

$$\overline{\text{SST}}_{t+1} = c_{\text{SST}} + \rho_c \overline{\text{SST}}_t + \beta_{\text{SST}} w_t m_t. \quad (9)$$

Without loss of generality, I define $\overline{\text{SST}}_t$ as the deviation from the pre-industrial baseline, so that:

$$\overline{\text{SST}}_{t+1} = \rho_c \overline{\text{SST}}_t + \beta_{\text{SST}} w_t m_t.$$

Similarly, annual disaster risk is similarly drawn from a distribution with mean $\bar{\delta}_t$ which is log-linear in the stock of atmospheric GHG:

$$\log \bar{\delta}_t = \tilde{c}_\delta + \tilde{\beta}_\delta \text{GHG}_t.$$

Simplifying similarly to Equation (9):

$$\log \bar{\delta}_{t+1} = \rho_\delta \log \bar{\delta}_t + \beta_\delta w_t m_t.$$

Conditional on global climate conditions, realized temperatures and logged disaster damages are Normally distributed and i.i.d.:

$$\begin{aligned} \text{SST}_t &\sim \mathcal{N}(\bar{\text{SST}}_t, \sigma^d) \\ \log \delta_t &\sim \mathcal{N}(\log \bar{\delta}_t, \sigma^d). \end{aligned}$$

Two sources of uncertainty are already present: internal variability, in the variability of annual temperature and disaster realizations given global climate conditions; and scenario uncertainty, in that emissions intensity evolves stochastically. In the following section, I will add a third source of uncertainty: climate model uncertainty, in which households do not directly observe the coefficients β_{SST} and β_δ , but instead must learn about them over time.

Altogether, this richer global climate process is as follows:

$\log w_{t+1} = \log w_t + g^w$	Global Energy Generation
$\log m_{t+1} = \log m_t - \beta_m w_t + \varepsilon_t^m$	Emissions Intensity
$\bar{\text{SST}}_{t+1} = \rho_{\text{SST}} \bar{\text{SST}}_t + \beta_{\text{SST}} w_t m_t$	Global Temperature
$\log \bar{\delta}_{t+1} = \rho_\delta \log \bar{\delta}_t + \beta_\delta w_t m_t$	Global Disaster Risk
$\varepsilon_t^m \sim \mathcal{N}(\mu_m, \sigma_m^2)$	Scenario Uncertainty
$\text{SST}_t \sim \mathcal{N}(\bar{\text{SST}}_t, \sigma_{\text{SST}}^2)$	Internal Temperature Variability
$\log \delta_t \sim \mathcal{N}(\log \bar{\delta}_t, \sigma_\delta^2)$	Internal Disaster Variability

4.2 Bayesian Updating of Climate Expectations

In order to incorporate model uncertainty—uncertainty over the coefficients β_{SST} and β_δ —I now consider rational Bayesian households who observe the climate process defined in Section 4.1. The households do not directly observe the coefficients β_{SST} and β_δ or the true means $\bar{\delta}_t$ and $\bar{\text{SST}}_t$. Instead they observe only the noisy realizations δ_t and SST_t . I assume that all households have common priors and common signals.

At the beginning of each period t , the household's information set

$$\mathcal{I}_t = \left\{ \hat{\mathbf{x}}_t^{\text{SST}}, \hat{\mathbf{P}}_t^{\text{SST}}, \hat{\mathbf{x}}_t^\delta, \hat{\mathbf{P}}_t^\delta \right\}$$

encodes a multivariate Normal prior

$$\mathcal{N}\left(\hat{\mathbf{x}}_t^{\text{SST}}, \hat{\mathbf{P}}_t^{\text{SST}}\right) \quad \text{over} \quad \begin{bmatrix} \overline{\text{SST}}_t \\ \beta^{\text{SST}} \end{bmatrix}$$

and a multivariate Normal prior

$$\mathcal{N}\left(\hat{\mathbf{x}}_t^\delta, \hat{\mathbf{P}}_t^\delta\right) \quad \text{over} \quad \begin{bmatrix} \log \bar{\delta}_t \\ \beta^\delta \end{bmatrix}.$$

I assume that these two multivariate priors are independent. The learning processes for β_{SST} and β_δ are identical. For brevity, I describe only the process for β_δ . Each period, the expected value $\bar{\delta}_t$ of disaster damages evolves and disaster damages themselves, δ_t , are realized, as described in Section 4.1. Households update their prior by observing δ_t and a Normally distributed news shock n_t^δ :

$$\begin{aligned} \log \bar{\delta}_{t+1} &= \rho_\delta \log \bar{\delta}_t + \beta_\delta w_t m_t \\ \log \delta_t &\sim \mathcal{N}(\log \bar{\delta}_t, \sigma_\delta^d) \\ n_t^\delta &\sim \mathcal{N}(\mu^\delta, \sigma_\delta^n). \end{aligned}$$

This is a linear Gaussian state space model. Assuming rational Bayesian learning, the posterior given emissions is linear in the shock realizations, and given by the Kalman filter.

In matrix form, the unobserved state evolves according to:

$$\underbrace{\begin{bmatrix} \log \bar{\delta}_{t+1} \\ \beta_\delta \end{bmatrix}}_{\mathbf{x}_{t+1}} = \underbrace{\begin{bmatrix} \rho_\delta & w_t m_t \\ 0 & 1 \end{bmatrix}}_{\mathbf{F}_t} \underbrace{\begin{bmatrix} \log \bar{\delta}_t \\ \beta_\delta \end{bmatrix}}_{\mathbf{x}_t}.$$

and shock realizations are generated according to:

$$\underbrace{\begin{bmatrix} \log \bar{\delta}_t \\ n_t \end{bmatrix}}_{\mathbf{z}_t} = \underbrace{\begin{bmatrix} 1 & 0 \\ 1 & 0 \end{bmatrix}}_{\mathbf{H}_t} \underbrace{\begin{bmatrix} \log \bar{\delta}_t \\ \beta_\delta \end{bmatrix}}_{\mathbf{x}_t} + \mathbf{v}_t$$

$$\mathbf{v}_t \sim \mathcal{N}(0, \Sigma_v).$$

Given the common prior for \mathbf{x}_t at the beginning of period t ,

$$\mathbf{x}_t \mid \mathcal{I}_t \sim \mathcal{N}\left(\hat{\mathbf{x}}_t^\delta, \hat{\mathbf{P}}_t^\delta\right),$$

the rational prior for \mathbf{x}_{t+1} at the beginning of period $t + 1$ is given by the Kalman filter:

$$\begin{aligned}\hat{\mathbf{x}}_{t+1}^{\delta} &= \mathbf{F}_t(\mathbf{I} - \mathbf{K}_t \mathbf{H}_t) \hat{\mathbf{x}}_t^{\delta} + \mathbf{F}_t \mathbf{K}_t \mathbf{z}_t \\ \hat{\mathbf{P}}_{t+1}^{\delta} &= \mathbf{F}_t(\mathbf{I} - \mathbf{K}_t \mathbf{H}_t) \hat{\mathbf{P}}_t^{\delta} \mathbf{F}_t' \\ \mathbf{K}_t &= \hat{\mathbf{P}}_t^{\delta} \mathbf{H}_t' (\mathbf{H}_t \hat{\mathbf{P}}_t^{\delta} \mathbf{H}_t' + \Sigma_v)^{-1},\end{aligned}$$

where \mathbf{K}_t is the optimal Kalman gain.

$$\log \delta_t \mid \mathcal{I}_t \sim \mathcal{N}(\hat{\mu}_t, \sigma_d + \hat{\sigma}_{\mu t}).$$

4.3 Quantification: Climate Process

The Intergovernmental Panel on Climate Change (IPCC) define greenhouse gas concentration scenarios (effectively emissions scenarios). They are labelled RCP x , where x is the level of radiative forcing (net energy transfer from space) per m^2 of the Earth's surface. Figure 11 shows these pathways. CMIP5 estimate projections of the response of local temperatures, measured in heating and cooling degree days, to global temperature change (Figure 1).

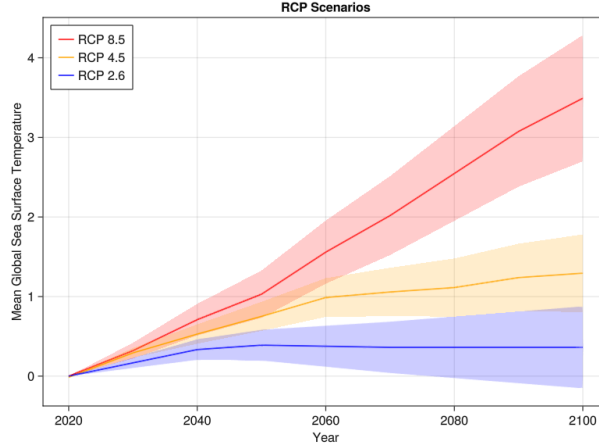


Figure 11

Representative Concentration Pathways (RCPs) from the IPCC Fifth Assessment Report (AR5). The RCPs are labelled by the level of radiative forcing (net energy transfer from space) per m^2 of the Earth's surface.

The IPCC identifies three sources of uncertainty over future climate damages: (1) internal variability: normal fluctuations in the climate system, which would occur even in the absence of climate change; (2) model uncertainty: uncertainty over the damages resulting from a given emissions scenario; (3) scenario uncertainty: uncertainty over the path of emissions.

I calibrate the free variables of the climate process are as follows. I set initial global energy generation,

Table 3: Calibrated Parameters, Auxiliary Climate Process

Parameter	Interpretation	Value	Target or Source	Moment	Value
w_0	Initial global energy generation	107 PWh	Global energy generation, 1900	107 PWh	
g^w	Global energy generation growth rate	0.0155	Growth rate of global energy generation, 1900-2020	0.0155	
m_0	Initial emissions intensity	0.358 t/MWh	Global emissions intensity, 2020	0.273 t/MWh	
β_m	Decline in emissions intensity	0.016	RCP4.5 annual emissions, 2100 (as median)	12.3 Gt	
σ_m^2	Variance of emissions intensity shock	0.40	RCP2.0/4.5/6.0 SST, 2100 (as quartiles)		
β_{SST}	Contribution of emissions to global temperatures	0.00053	" "		
ρ_{SST}	Natural rate of temperature regression	0.93	" "		
β_δ	Contribution of emissions to disaster damages	0.051	Increase in disaster damages 2020-2050 (Bates et al., 2021)	26.4%	
ρ_δ	Natural rate of disaster damage regression	0.98	Homeowners insurance premiums		

All moments are either unitless or in units of decade⁻¹. Each parameter influences all moments; I merely report the most directly influenced moment for each parameter.

w_0 , to global energy generation in 1900. I set the growth rate of global energy generation, g^w , to the growth rate of global energy generation between 1900 and 2020. I set initial emissions intensity, m_0 , to match average global emissions intensity in 2020. I set the parameter controlling the decline in emissions intensity, β_m , to match model-predicted median annual emissions in 2100, $w_{2100}m_{2100}$, conditional on 2020 emissions, to 2100 emissions in the RCP4.5 scenario.

I jointly set the variance of the emissions intensity shock, σ_m^2 ; the contribution of emissions to global temperatures, β_{SST} ; and the natural rate of regression of temperatures to the pre-industrial baseline, ρ_{SST} . I match the first, second, and third quartiles of global temperatures in 2100, conditional on 2020 emissions, to the RCP2.0, RCP4.5, and RCP6.0 scenarios.

I set the contribution of emissions to disaster damages, β_δ , to match the increase in disaster damages between 2020 and 2050 predicted by the model of Bates et al. (2021), as reported by Wing et al. (2022). I estimate the natural rate of regression of disaster damages to the pre-industrial baseline, ρ_δ , using data on historical homeowners insurance premiums in Appendix B.

4.4 Quantification: Model Uncertainty

I use historical data on homeowners insurance premiums and losses to estimate market-relevant internal variability and model uncertainty. Homeowners insurance contracts are one-year contracts, representing a plausibly static decision on the part of the insurer. Using aggregate accounting data, I back out anticipated annual losses from storm damage, given insurers' beliefs and information sets, in each year.

In order to measure uncertainty, I use the responsiveness of premiums (encoding anticipated losses) to realized losses. Intuitively, the less certain insurers are in their climate beliefs, the more we would expect them to adjust their premiums in response to realized losses.

I model insurer's beliefs as arising from a Bayesian learning process. I then use data on premiums and losses to estimate the parameters of this process. Essentially, I am learning from the observed learning behavior of insurers. I show that the specific procedure I employ, which resembles a nested Kalman filter, can be constructed at a high level of generality.

As the procedure for estimating the Bayesian model is quite long and complex, and yields few insights of interest regarding the unequal climate impacts which are the primary focus of this study, I move it to Appendix B. Table 4 reports the result of the estimation.

Variable	Estimate
σ_δ^n	0.21306
σ_δ^d	0.28874
ρ	0.98
T_0	1965.87

Table 4: Results of state space estimation. Point estimates are by maximum likelihood.

5 Calibration

It remains to set the climate-unrelated parameters of the full model. Because the goal is to explore the implications of the model for the period 2020-2100, I calibrate the model's stationary steady state to be consistent with key features of the U.S. economy in the early 1990s. As described in Section 2.6, this is the initial steady state in which climate change unexpectedly begins.

I choose the early 1990s to achieve a balance between, on one hand, capturing the effects of anticipatory adaptation to climate change and, on the other hand, capturing factors which shape current housing markets but are not incorporated in the model. Calibrating the model to a more recent steady state allows for the initial conditions to be more similar to the current economy, but allows for less pre-2020 adjustment by households in anticipation of climate change.

I primarily calibrate the model primarily using indirect inference. I match moments computed from the 1990 U.S. Census, specifically the 5% Public Use Microdata Sample (PUMS) and the 1992 Survey of Consumer Finances (SCF).

The parameters of the model can be divided into four categories: location-level parameters, the parameters of the income process, the initial wealth distribution, and all other parameters.

Each location is calibrated to data on a single Public Use Microdata Area (PUMA), the smallest spatial

unit available in the 1990 PUMS. I plug in housing price estimates from PUMS, solve for local rents and populations in spatial equilibrium, and calibrate location-specific amenities and labor productivity shifters to match empirical location populations and mean incomes from PUMS. These estimates are independent of local housing supply elasticities. I assign these externally using the spatially-heterogeneous estimates of Saiz (2010).

The labor income process is calibrated by quantifying an annual AR(1) process on labor, welfare, and pension income from the 1989 and 1990 Panel Study of Income Dynamics (PSID), then calibrating a decadal AR(1) income process to the moments of the annual process.

I parameterize the initial wealth distribution to be log-uniform within each income quartile, yielding the five quartile boundaries (including the minimum and maximum wealth) as the free parameters. I set the minimum to \$1 and the remaining four by indirect inference, matching the mean and inner three quartiles of overall net worth in the 1992 SCF.

To quantify non-spatially-varying parameters, I use a combination of indirect inference, external estimates, and standard values. Seven parameters are calibrated by indirect inference. Abstractly, I define seven moments and find values for these seven parameters such that the simulated moments equal the empirical moments.

Concretely, I assign to each parameter a corresponding moment which the model suggests should particularly informative about that parameter. I do this for the parameters of the wealth distribution, the non-spatially-varying parameters, as well as the location-specific amenities and productivity shifters.²¹ I then simply guess all parameters at once, compute simulated moments, then update each parameter guess using only the difference between the simulated and empirical moments associated with that parameter, and repeat until all simulated moments equal their empirical counterparts (within some tolerance).

That is, I essentially find the parameters by gradient descent, where I set every derivatives of a moment with respect to parameters to zero except for the hypothesized “relevant” parameter. The fact that this process converges provides support for the hypothesis that the chosen moments are indeed informative about their corresponding parameters.

The precise meaning of statements of the form, “I set Parameter X to match Moment Y,” is that Parameter X is associated with Moment Y but all parameters are estimated simultaneously according to the above procedure.

²¹As an optimization, I also treat local rents as parameters, with the market clearing condition as the “associated moment.” This removes the need to solve for equilibrium rents for every parameter guess.

5.1 Spatial Parameters

I choose the 1990 Public Use Microdata Area (PUMA) as my spatial unit. These are the units reported in the 1990 U.S. Census. I use the $N = 1713$ PUMAs which cover the contiguous U.S. completely. A PUMA is an area with 1990 population between 100,000 and 200,000, generally following the boundaries of Metropolitan Statistical Areas (MSAs) where applicable.

For each location ℓ , I set the housing price level²² q_ℓ to the value of a typical owner-occupied two-bedroom home in the 1990 PUMS.²³ By indirect inference, I set the local “amenity value” or exogenous quality of life shifter $\bar{\alpha}_\ell$ to match the population of location ℓ in the 1990 PUMS. By indirect inference, I set the local labor productivity shifter \bar{A}_ℓ to match the mean earnings among the working-age population in location ℓ in the 1990 PUMS.

In equilibrium, these imply a value in each location for the quantity of housing H_ℓ and the rent level²⁴ ρ_ℓ , which are untargeted. I explore their fit in Section 5.5.

After calibrating the model, the elasticities of local housing supply β_ℓ is not separately identified from the housing price shifters Π_ℓ . In steady state:

$$q_\ell = \Pi_\ell H_\ell^{\beta_\ell}.$$

To quantify β_ℓ , plug into the above the estimated prices q_ℓ from PUMS and the model-predicted equilibrium H_ℓ in each location. I then use the estimates of Saiz (2010) to set β_ℓ for each location ℓ and solve for Π_ℓ . The estimates of Saiz (2010) are at the level of MSAs, which generally nest PUMAs. Details of the imputation procedure are in Appendix E.

5.2 Initial Wealth Endowments

By indirect inference, I set the distribution of initial wealth endowment (at age 20) to match the mean and quartiles of net worth in the SCF. A household is equally likely to be born in each quartile. Conditional on quartile, initial wealth endowment is log-uniform. The minimum initial wealth endowment is \$1. I set the maximum initial wealth endowment to match the empirical mean of net worth.

5.3 Non-Spatial Parameters

The non-spatial parameters of the model determine preferences, the lifecycle income process, initial wealth endowments, housing investment and maintenance costs, and migration costs. In addition to Census data, I also use data from the 1992 Survey of Consumer Finances (SCF).

²²As I am calibrating a steady-state version of the model, I omit time t subscripts.

²³See Appendix E for the precise construction of this variable.

²⁴In units which correspond to the typical owner-occupied two-bedroom home.

5.3.1 Lifecycle

One model period represents ten years. Households are born at age 20 and die at age 80.

5.3.2 Preferences

By indirect inference: I set the weight of housing in consumption, γ , to match the median rent-to-income ratio among renters in the 1990 Census; I set the strength of the bequest motive, Q , to match the ratio between overall mean wealth and mean wealth of households with a head between 70 and 80; and I set the elasticity of substitution between housing and goods consumption, $1/\sigma$, to match the reduced form relationship β_{RTI} , across locations, between the housing asset price level q_ℓ and median rent-to-income ratio:²⁵

$$\text{RTI}_\ell = \alpha_{\text{RTI}} + \beta_{\text{RTI}} \log q_\ell + \varepsilon_\ell.$$

where RTI_ℓ is the median rent-to-income ratio in location ℓ .

Externally, I set the elasticity of intertemporal substitution to $1/\eta = 2.0$ as in Kaplan et al. (2020).

5.3.3 Housing

I set the interest rate on mortgage borrowing, r_m , to match the ratio between the mean wealth of homeowners to overall mean wealth. I set the baseline cost of maintaining a rental property to match the homeownership rate. I set the excess maintenance and administrative cost on rental properties, $\chi^{\text{let}} - \chi^{\text{live}}$, to match the homeownership rate.

Externally, I set the transaction cost for housing assets, ϕ , to 7% as in Kaplan et al. (2020). I set the maximum loan-to-value ratio of a mortgage, κ , to 80%. I set χ^{live} , the baseline cost of maintaining an owner-occupied home, to \$1,000 annually.

5.3.4 Migration

I parameterize the utility migration cost,²⁶ $F^u(\ell', \ell)$, as linear in the distance $d(\ell', \ell)$ between the source location ℓ and destination location ℓ' :

$$F^u(\ell', \ell) = \overline{F^u} + F^{u,\text{dist}} d(\ell', \ell).$$

I set $\overline{F^u}$ to match the share of households who move across PUMAs each decade. I set $F^{u,\text{dist}}$ to match the share of households who move across states each decade.

²⁵Ideally, I would regress on the housing rent level, but I do not observe this in the data.

²⁶No aspect of the model solution depends on any particular functional form, however. In a future version, I plan to calibrate migration costs for each pair of locations to match data on bilateral migration flows.

Table 5: Units

Quantity	Unit
Location	1990 Public Use Microdata Area (PUMA)
Time	10 years
Housing	Typical two-bedroom owner-occupied home
Numeraire Good	Thousand 2020 USD (\$1,000)
Distance	Kilometers (km)
Temperature	Degrees Celsius (°C)

Units used throughout the quantification, unless otherwise specified. “Monetary” values such as income and monetary moving costs are paid in the form of the numeraire good, which are expressed in units of one thousand 2020 USD.

Externally, I set the monetary cost of moving to \$13,260 (2020 USD) as in Giannone et al. (2023).

5.4 Calibration Result

Table 5 lists the units that all quantities are expressed in. The model is just-identified. That is, I successfully match all targeted moments exactly. Table 6 Figure 12 describes the estimated local amenity values across the U.S. Figure 13 describes the estimated local productivity shifters across the U.S. To illustrate the degree of spatial heterogeneity, Figure 14 describes estimated local amenity values for six cities, and Figure 15 describes local productivity shifters around New York City at various scales.

5.5 Model Fit

Local rent levels and housing stocks are not targeted in the calibration, but arise in the model equilibrium. Figure 16 shows that rent levels vary with housing prices, as both are driven by local amenity values, productivities, and housing supply elasticities. Furthermore, Figure 17 reveals that the model reproduces a key feature of the data: the price-to-rent ratio is higher in locations with higher housing prices. This is primarily driven by the fact that a greater concentration of wealth in more expensive locations creates greater demand for rental real estate assets, decreasing equilibrium rents. Second, a small proportion of this effect is due to a particular modeling choice: the wedge between the maintenance cost of rental housing and owner-occupied housing is a fixed cost per unit of housing, so it is relatively lower in locations with higher housing prices. However, in the calibrated model maintenance costs account for only between 5% and 25% of rent and cannot account for the large variation in price-to-rent ratios.

Table 6: Non-Spatially-Varying Parameters

Parameter	Interpretation	Value	Target or Source	Moment Value
Lifecycle:				
a_{\max}	Length of adult life	6		
Preferences:				
γ	Taste for housing	0.007	Median (renter) rent-to-income ratio	0.23
$1/\sigma$	Elasticity of Substitution (goods vs. housing)	0.87	Rent-to-income sens. to housing price	0.011
$1/\eta$	Elasticity of intertemporal substitution	0.5		
Q	Bequest motive	4.3	Mean wealth ratio oldest-to-overall	1.62
Housing:				
r_m	Mortgage interest rate	0.80	Mean wealth ratio homeowners-to-overall	1.52
ϕ	Transaction cost	0.07	Kaplan et al. (2020)	
χ^{let}	Rental baseline maintenance cost	21.3	Homeownership rate	0.68
κ	Maximum loan-to-value ratio	0.8		
χ^{live}	Owner-occupied baseline maintenance cost	10.0		
Migration:				
\bar{F}^u	Utility cost of migration	3.51	Share of households moving across PUMAs	0.40
$F^{u,\text{dist}}$	Utility cost of migration per km	0.001	Share of households moving across states	0.22
F^m	Monetary cost of migration	13.3	Giannone et al. (2023)	

All moments are either unitless or in units of decade⁻¹. Each parameter influences all moments; I merely report the most directly influenced moment for each parameter.

Calibrated Amenities

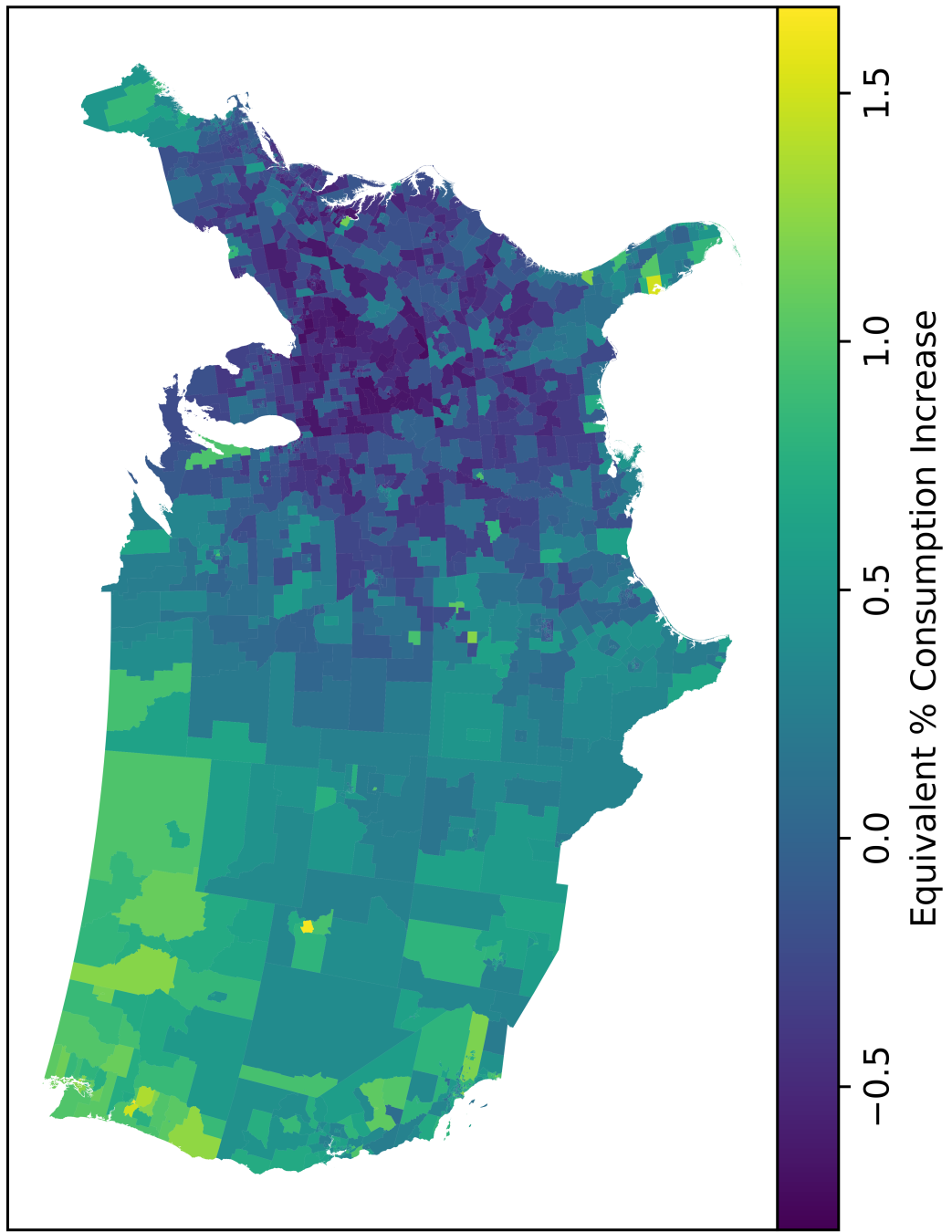


Figure 12: Estimated Amenity Values

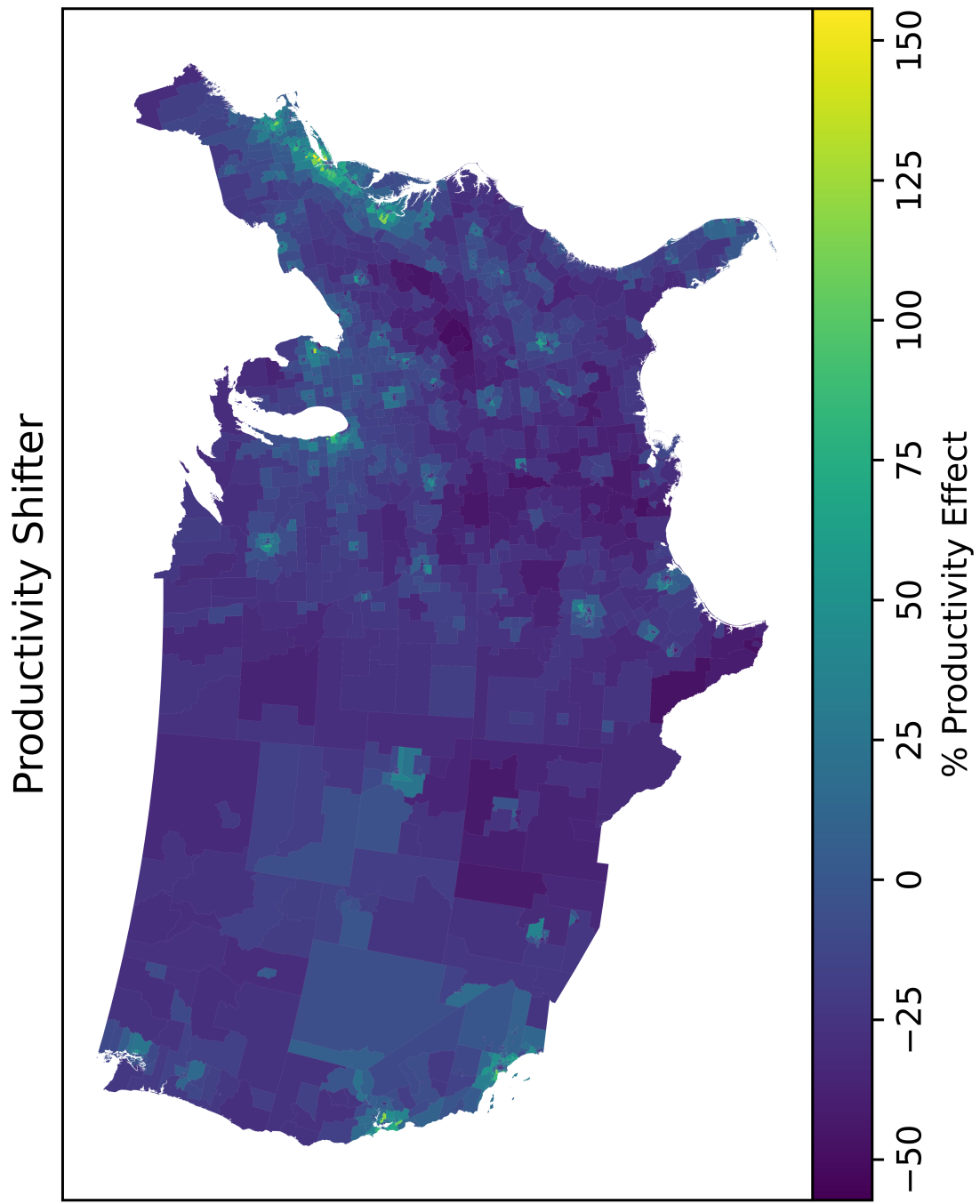


Figure 13: Estimated Productivity Shifters

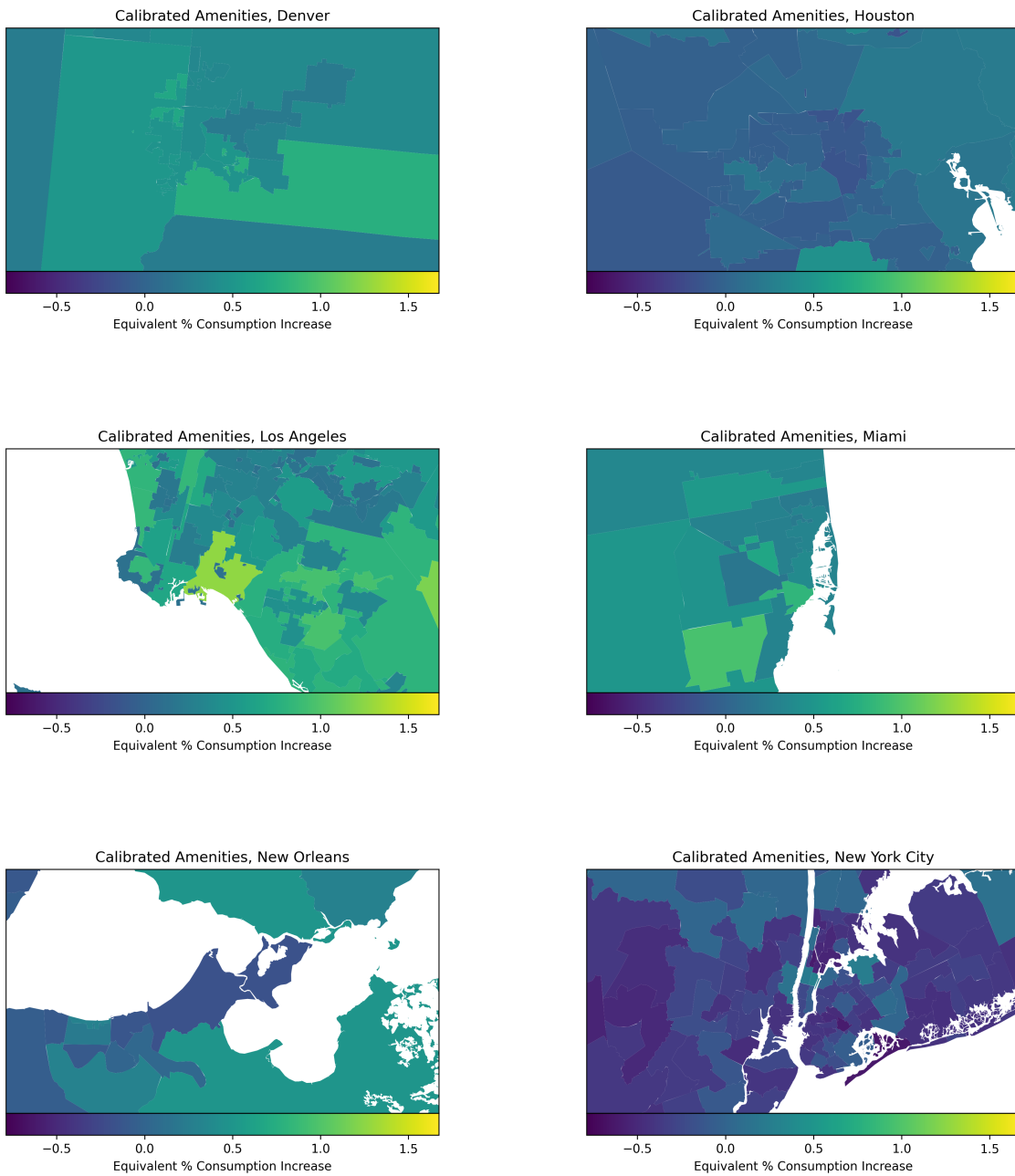


Figure 14: Calibrated Amenities by City

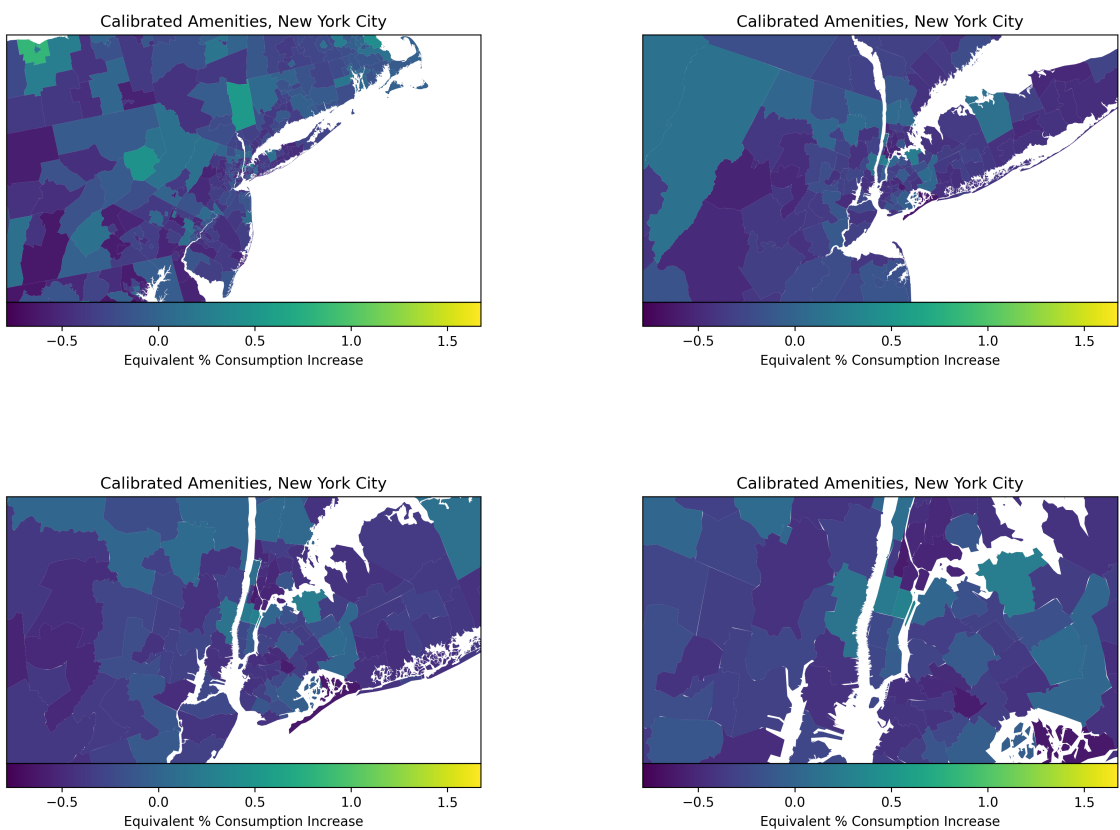


Figure 15: Calibrated Amenities Around New York City

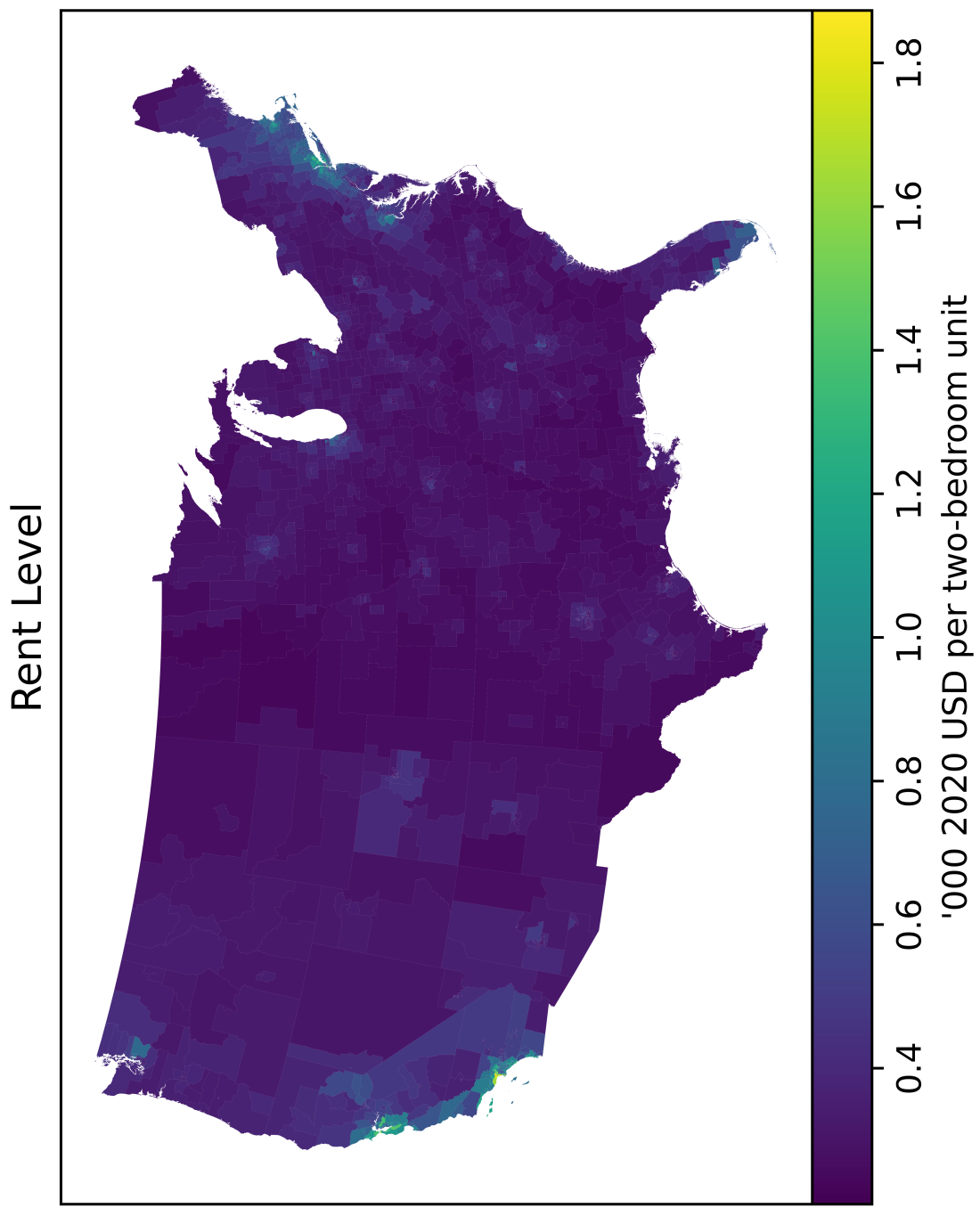


Figure 16: Equilibrium Rent Level

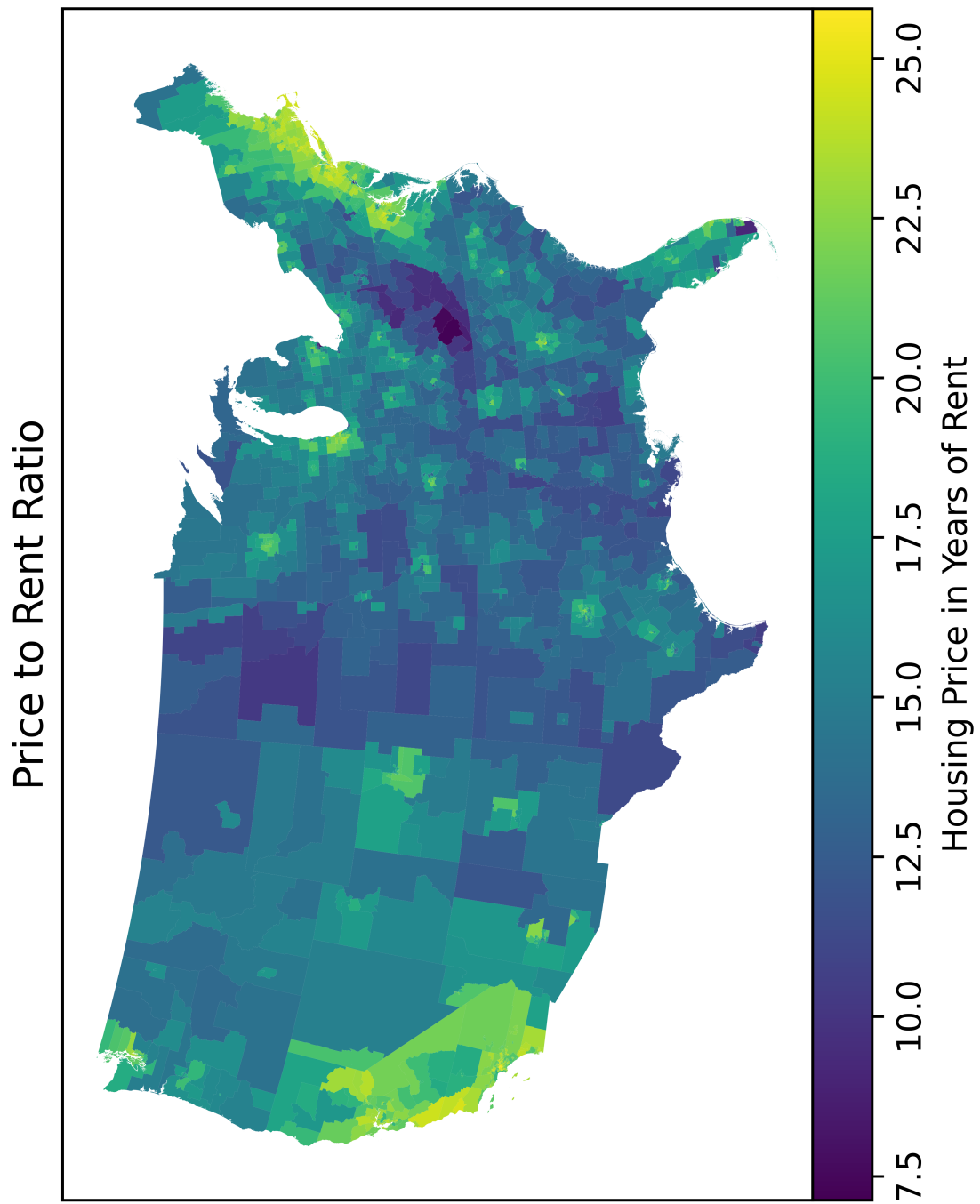


Figure 17: Equilibrium Price to Rent Ratio

6 Inequality in Welfare Losses from Climate Change

In this section, I examine inequality in the welfare losses from climate change in the U.S.—overall, within locations, and between locations. The first key contribution of this model is to incorporate housing wealth, which is determined by forward-looking equilibrium housing prices. The second key contribution is to incorporate climate uncertainty and its equilibrium impact on house prices. This requires finding the global solution of the dynamic spatial equilibrium model under aggregate uncertainty.

When household wealth depends on forward-looking housing prices, neither migration nor anticipation can greatly ameliorate the spatially-unequal impacts of climate change. Although adding migration to a version of the model without migration or homeownership does mitigate spatial inequality in climate damages, this is undone by adding homeownership. To quantify the impact of housing wealth, I compare the full model to a version of the model in which households rent housing from an absentee landlord.

Forward-looking housing prices cause news about future climate change to have immediate unequal wealth impacts at the time that the news is revealed, though these wealth impacts do reduce overall wealth inequality. However, uncertainty about future climate change causes ongoing regressive welfare impacts through increasing housing rent. Landlords effectively charge renters for the risk that landlords adopt by holding risky housing assets. Wealthier landlords profit from the reduced willingness of less wealthy landlords to invest in real estate. To quantify the effects of uncertainty, I compare the global solution to a version of the model with perfect foresight.

Finally, there is one more key way in which expectations shape the distributional consequences of climate change. With homeownership, if households systematically underestimate the severity of climate change, then this causes a progressive distributional impact to be realized during the climate transition when the news is revealed that climate change will be more severe than anticipated. This negative climate news shock causes a reduction in the value of housing assets, which are concentrated in the portfolios of wealthier households.

6.1 Inequality in Welfare Losses from Climate Change

In this section, I consider an extreme form of anticipation: a sudden switch from widespread denial to widespread acceptance of climate change. The economy begins in steady state when the stochastic climate transition described in 2.4.2 unexpectedly begins. All households immediately internalize the parameters of the climate process. In a future version, I plan to explore the implications of a more gradual transition from denial to acceptance. Nevertheless, the sudden switch should capture the full magnitude of the price changes resulting from the climate news shock, which in reality would likely unfold more slowly.

With anticipation, welfare losses from climate change manifest in two broad ways. First, when news of

climate change is revealed, households are immediately affected by the instantaneous adjustment of housing prices. Second, young households born during the climate transition are, on average, worse off than if climate change had not occurred. I consider each in turn.

6.1.1 Immediate Welfare Impacts of News Shock

Figure 18 describes welfare losses from the unexpected start of the climate transition, relative to the continuation of the steady state. For each household, I compare the value function at the beginning of the first period of the climate transition with the steady state value function.

This measure combines two effects, however. First, the effect of future climate damages; second, the wealth effect of the climate news shock, operating through housing prices. To isolate the latter, I consider, for each individual household,²⁷ the welfare impact of adjusting that household's liquid savings in order to exactly undo the effect of the news shock on their net worth through housing assets. That is, for each household I compute the welfare impact of a (possibly negative) news shock equal to the negated change in the value of their housing asset portfolio. Figure 19 plots the distribution of wealth impacts as a percentage of household portfolio value. Figure 20 plots the distribution of these welfare impacts.

Table 7 decomposes the variance in the immediate welfare impacts plotted in Figure 18 into within-location and between-location components. Approximately 65% of the variance is within-location.

Figure 21 maps spatial inequality in welfare losses from the unexpected start of a climate transition. Figure 22 maps the immediate house price changes resulting from the news shock. Over all areas where prices increase, the value of the housing stock increases by \$996bn. Over all areas where prices decrease, the value of the housing stock decreases by \$1.61tn. Overall, \$618bn in housing value is lost, and \$996bn in housing value is effectively transferred from negatively-affected areas to mildly- and positively-affected areas.

²⁷That is, I do not consider a widespread policy of compensation for housing wealth losses.

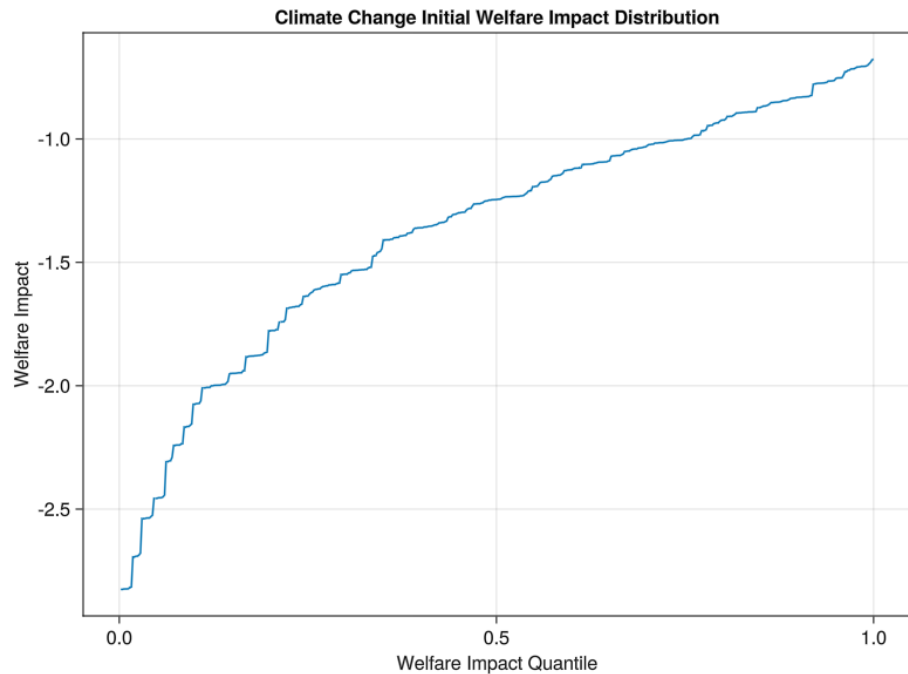


Figure 18

Initial welfare losses from the unexpected start of the climate transition, relative to steady state. Overall, welfare losses are equivalent to a \$2.8tn wealth transfer from more-harmed to less-harmed households.

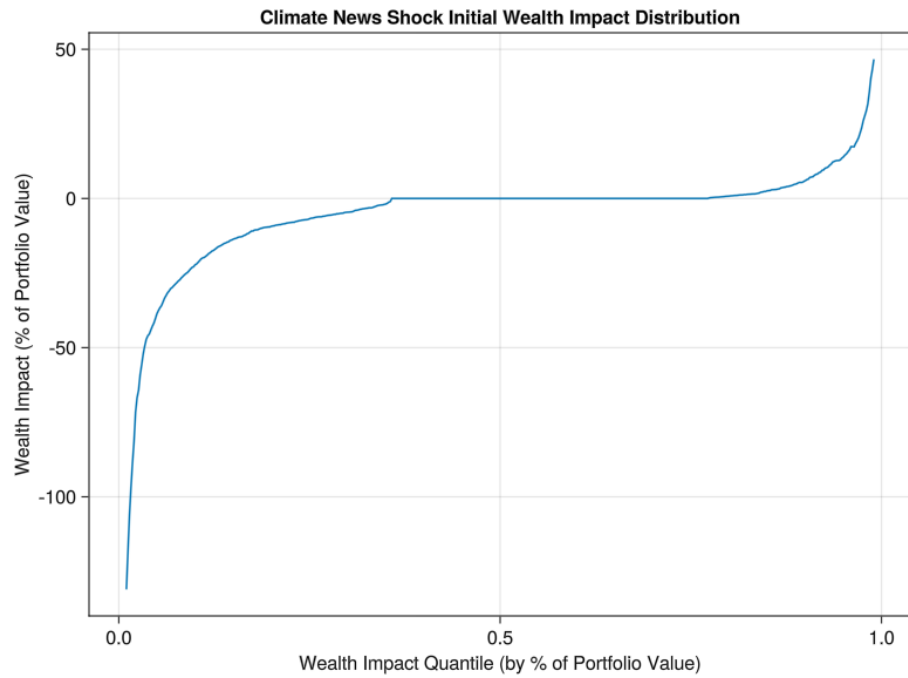


Figure 19

Initial wealth impacts due to house price adjustment from the unexpected start of the climate transition, as a percentage of household portfolio value.

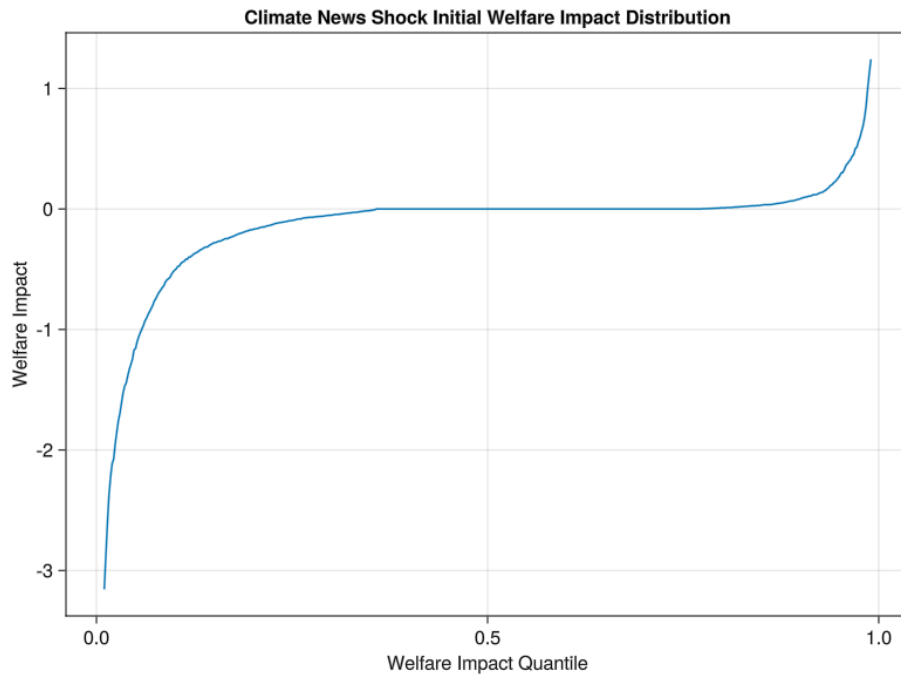


Figure 20

Initial welfare impacts due to house price adjustment from the unexpected start of the climate transition, relative to having additionally received or paid a wealth transfer exactly offsetting the wealth shock from housing assets.

Table 7: Initial Welfare Impact: Variance Decomposition

Variance Component	Value
Overall	0.018
Within-Location	0.012
Between-Location	0.006

Decomposition of variance in welfare effects of house price adjustments following the unexpected start of climate change.

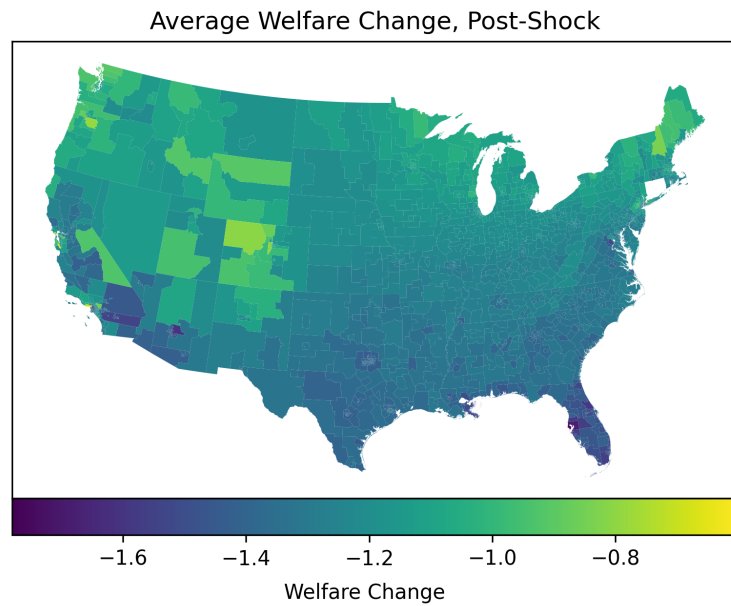


Figure 21: Average welfare reduction resulting from the unexpected start of the climate transition.

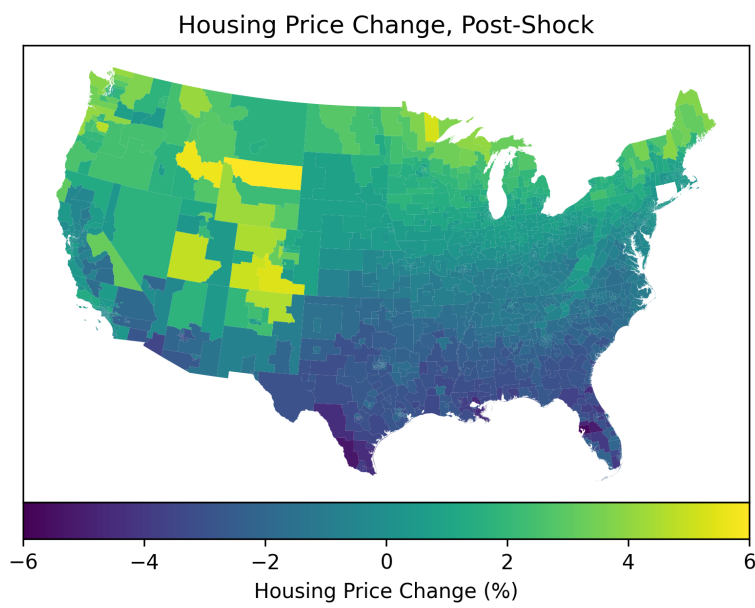


Figure 22: Immediate housing price changes resulting from a news shock, in an initial steady state, that an unexpected climate transition is beginning.

6.1.2 Welfare Impacts Along the Climate Transition

Figure 23 describes welfare losses for households born sixty years after the beginning of the climate transition, relative to the continuation of the steady state. For each household, I compare the value function at the first period of their life with the initial value function of a household born into the stationary steady state.

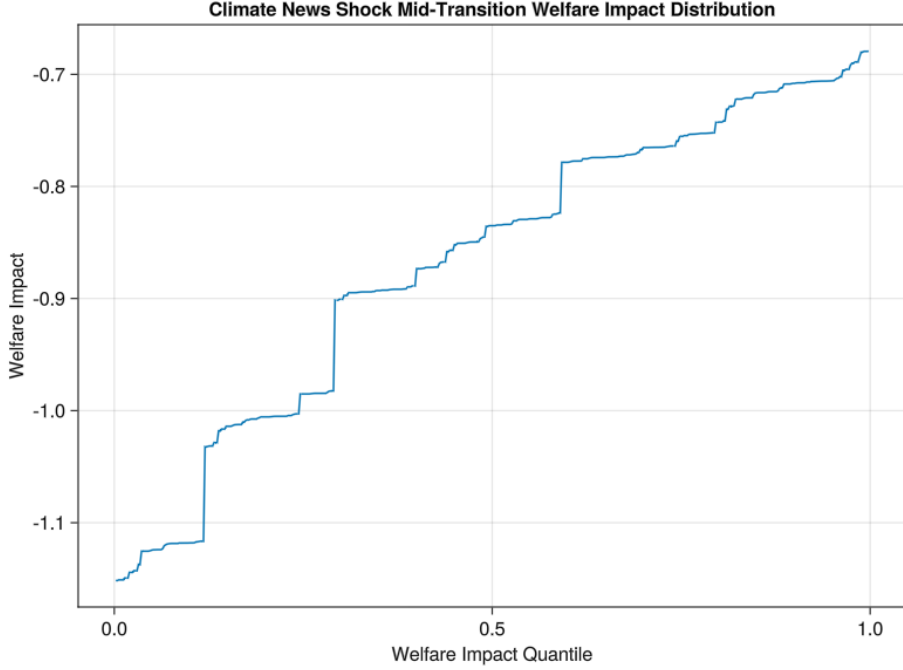


Figure 23

Welfare losses 60 years after the beginning of the climate transition. Welfare of a 20-year-old household born during the climate transition is compared with welfare of a 20-year-old household born into the steady state.

6.2 Anticipation, Forward-Looking Prices, and Uncertainty

In the calibrated model, whether climate change exacerbates or alleviates wealth inequality hinges on whether households over- or under-estimate the severity of climate change and on how uncertain they are in their assessment. That is, the sign of the distributional impact depends on both the mean and the variance of climate expectations. First, the mean: the more that households systematically underestimate the severity of climate change, the more climate change reduces wealth inequality through reducing the value of housing assets (to which wealthier households are more highly exposed). Second, the variance: the more that households are uncertain about the severity of climate change, the more climate change exacerbates wealth inequality through raising risk premia on housing assets. Higher risk premia primarily take the form of higher rent-to-price ratios on housing assets, benefiting the more risk tolerant wealthier households but harming less wealthy households who are more risk-averse and more likely to be renters.

Note that these results depend crucially on having the global solution of the model. If we were studying a deterministic transition, there would be no uncertainty, no risk premium, and no regressive distributional impact of the risk premium.

6.3 Distributional Consequences of Under and Over-estimating Climate Change

If households underestimate the severity of future climate change, then the news that climate change will be more severe than expected will eventually arrive as a negative climate news surprise. This reduces the average value of housing assets, which are concentrated in the portfolios of wealthier households, reducing overall wealth inequality. However, because some locations experience an increase in housing values, a subset of wealthy households benefit substantially from a negative climate news surprise.

Figure 24a describes an illustrative scenario. I consider three paths from the distribution of climate paths defined by the stochastic process in Section 2.4.2. The first is the median or “no surprise” path in which the realized value of the climate shock drawn each period is equal to 0. This path approximately corresponds to the RCP4.5 scenario.

$$\varepsilon_t^{m,\text{median}} = 0 \quad \forall t.$$

The second is the “negative surprise in 2050” path, in which the realized value of the climate shock drawn each period is zero, except for the shock drawn in 2050, ε_{2050}^m , which is equal to the 95th percentile of the shock distribution (implying higher future temperatures). The third path is the “positive surprise in 2050” path, in which all shocks are zero, except that ε_{2050}^m is equal to the 5th percentile of the shock distribution (implying lower future temperatures).

The welfare of wealthier households is more sensitive to climate surprises than the welfare of less wealthy households. To understand why, I shut down one channel at a time: first, uncertainty; second, exposure of house prices to climate surprises. After shutting down exposure of house prices to climate surprises, the correlation between wealth and climate sensitivity flips: climate sensitivity is then decreasing in wealth.

To shut down uncertainty, I consider a model in which households believe that they have perfect foresight about the climate process and that the transition will effectively be deterministic along the median path. The positive or negative surprise in 2050, if it occurs, is fully unexpected. Following the surprise, households believe that the new path is deterministic. I start this model from the same initial 1990 steady state as the stochastic model, but instead of shocking this model into the full stochastic climate process, I shock it into the median path of the climate process with perfect foresight.

Figure 24b plots, in solid lines, the welfare impact of the climate surprise illustrated in Figure 24a, as a function of wealth, shutting down uncertainty. That is, until 2050, I effectively study a deterministic transition. Until 2050, households believe that they deterministically on the median path.

For each wealth group, I plot the value at the beginning of 2050 under the positive (blue) and negative (red) surprises, relative to the no-surprise scenario. Wealthier households benefit more from the positive surprise and are more harmed by the negative surprise. The relationship between wealth and climate sensitivity is positive.

To quantify the contribution of housing wealth to this positive wealth-to-climate-sensitivity relationship, we can consider the case in which housing prices are unaffected by the surprise. That is, we ignore market clearing conditions, and simply impose exogenously that house prices along the new path are equal to what equilibrium house prices would have been along the old path. The climate surprise still affects local labor productivity, amenities, energy costs, and disaster risk. These no-price-change shock scenarios can be understood as the combination of a climate shock with a government policy maintaining house prices at the previously anticipated levels through constructing and selling homes below cost (if market prices are too high) or purchasing and demolishing homes (if market prices are too low).

The resulting welfare effects, along the wealth distribution, are plotted in Figure 24a in dashed lines. Shutting down house price exposure to the climate surprise, the wealth-to-climate-sensitivity relationship becomes negative, illustrating that the higher climate sensitivity of wealthier households is due to their exposure to housing assets.

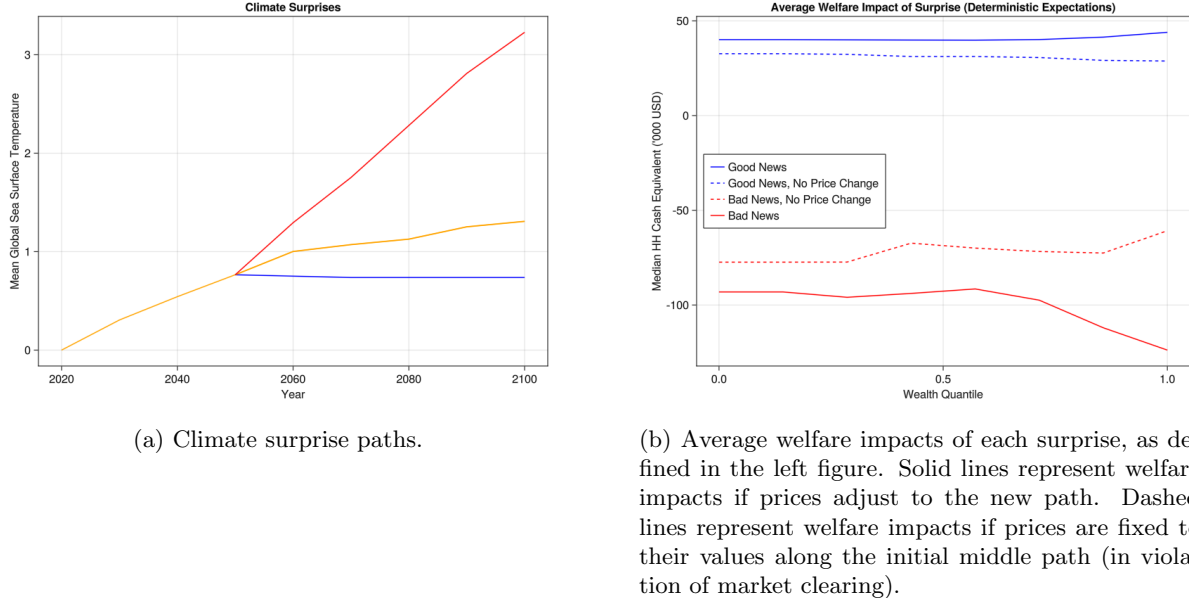


Figure 24

6.4 Distributional Consequences of Climate Uncertainty

We can understand the effect of climate uncertainty on wealth inequality by comparing the global solution of the model with aggregate climate uncertainty (the “Stochastic Model”) with a model of perfect foresight

in which the transition is effectively deterministic (the “Deterministic Model”).²⁸ In particular, consider the median path illustrated in Figure 24a. This arises as one possible realization of the full stochastic model. Consider now a deterministic model²⁹ in which households expect this median path to occur with certainty.

Each model begins in a stationary steady state representing the year 1990, then is hit by the news shock that a (stochastic or deterministic) climate transition is beginning. Figure 25 illustrates how average welfare varies by wealth percentile in the stochastic and deterministic models 30 years after the beginning of the climate transition.

The difference between the two models is climate uncertainty. If we shut down uncertainty (the “Deterministic Model”), then the welfare of households in the lower half of the wealth distribution is lower than in the model with uncertainty (the “Stochastic Model”). This regressive distributional consequence of climate uncertainty is equivalent to a \$94bn wealth transfer from the bottom half of the wealth distribution to the top.³⁰

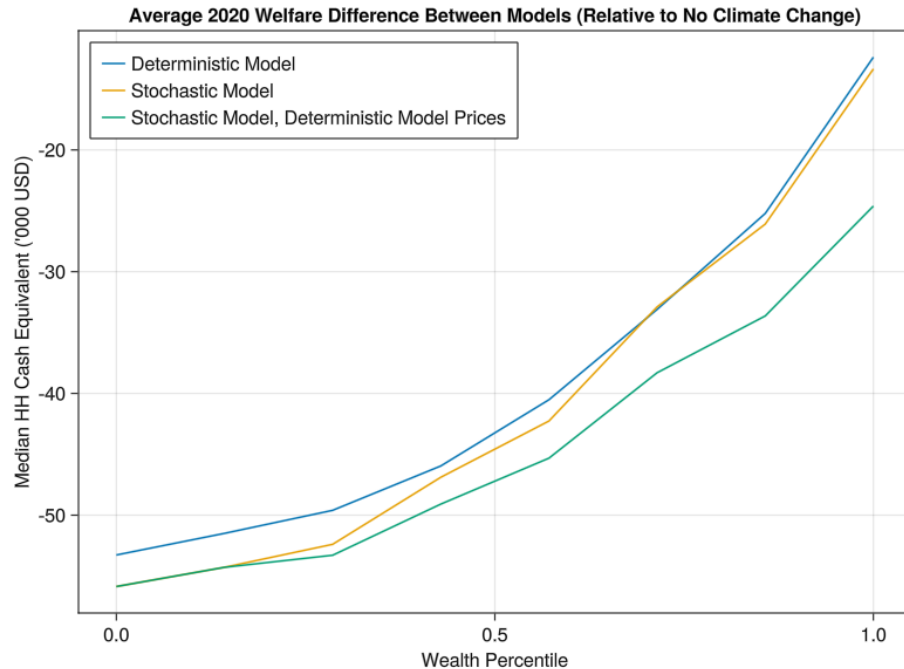


Figure 25: Welfare, relative to the no-climate-change stationary steady state, along the wealth distribution, in 2020, given the observed 1990-2020 climate realizations. The full stochastic model is shown, as well as a “deterministic model” under which the climate evolves according to the median path of the climate process with certainty, and a “stochastic model with deterministic prices” under which the climate evolves according to the full climate process, but prices are deterministically set to their path under the deterministic model (in violation of market clearing).

²⁸The distinction between these two models is one of household expectations, not that nature is somehow “more stochastic” in the global solution.

²⁹The same model generating the solid lines in Figure 24b.

³⁰I choose to focus on the relationship between welfare and wealth quantile as my measure of wealth inequality. The alternative would be to construct a price index for each simulated period, but this comes with the challenge that relative housing and goods prices vary across time as well as space and affect renters and homeowners differently.

To understand what is driving this regressive distributional effect of climate uncertainty, I shut down the exposure of house prices to climate uncertainty. In order to do this, I define a model in which households still face uncertainty over climate impacts on productivity, amenities, energy costs, and disaster risk, but house prices are exogenously constrained, no matter the realization of climate shocks, to equal the value they would have taken in the deterministic model.³¹ Figure 25 displays wealth inequality in this “Stochastic Model with Deterministic Model Prices,” compared to the Stochastic Model and the Deterministic Model. Wealthier households are worse off than they were in the stochastic model, but poorer households are unaffected on average, indicating that the uncertainty in housing prices in the Stochastic Model actually benefits richer households. This is due to an endogenous risk premium on housing assets that arises under aggregate climate uncertainty.

Figure 26 displays the paths of average house prices, across all locations, under the deterministic model and under the stochastic model. In the deterministic model, housing prices are an average of 1.16% higher in 2020. Note that the difference narrows over time, as uncertainty resolves. This also hints at the potential role of overconfidence in shaping economic climate outcomes. When markets are overconfident in their climate projections, risk premia will be smaller. Prices will be closer to the deterministic case, and the impacts of surprises will be closer to those described in Section 6.3.



Figure 26: Prices along the median path, under both the stochastic and deterministic models. In the stochastic model, expectations are that the climate will follow the process calibrated in Section 4. In the deterministic model, expectations are that the climate will deterministically follow the median path.

³¹As before, market clearing conditions will not hold in this scenario.

7 Conclusion

How large are inequalities in the welfare effects of climate change across households? I study how homeownership shapes the answer to this question by building and quantifying a dynamic spatial equilibrium model of the contiguous U.S. with 1713 locations. In the model, heterogeneous households make forward-looking consumption-savings, migration, and real estate investment decisions which, in aggregate, determine spatially heterogeneous housing prices. Crucially, housing prices both reflect expectations about future climate change and determine an empirically realistic proportion of household wealth.

With homeownership, inequality in the welfare impacts of climate change is large. Negative climate news shocks are progressive by wealth but climate uncertainty induces ongoing regressive wealth transfers. In response to a change in expectations from widespread climate denial to widespread climate acceptance, this inequality in welfare impacts is equivalent to a \$2.8tn wealth transfer from more-harmed to less-harmed households or a \$94bn wealth transfer from less-wealthy to more-wealthy households. In contrast to a model without individual housing asset ownership, migration adaptation does not substantially ameliorate spatial inequality in climate damages. Instead, households in severely-affected regions, whether or not they are actually displaced, suffer large climate-induced losses in housing wealth. In total, the spatially-heterogeneous adjustment of housing prices to the climate news shock is equivalent to a transfer of almost \$1tn in housing wealth from households in more-harmed to less-harmed regions.

In contrast to a model without housing wealth, anticipation does not greatly reduce spatial inequalities in climate damages. Instead, the primary effect is simply that unequal damages happen earlier, at the time that negative climate news is revealed. Furthermore, with anticipation and housing wealth, uncertainty introduces regressive wealth transfers. Climate risk causes households to be less willing to own rental housing, raising rent and expected returns on housing. Among households who do own housing, wealthier households are more willing to bear this risk, benefiting from the higher risk premia required by marginal, less-wealthy landlords. Less-wealthy renters are hurt by higher rents. Altogether, the regressive welfare impact of uncertainty is equivalent to a transfer of \$94bn from the bottom half of the wealth distribution to the top half, relative to a model with perfect foresight. The analysis of climate uncertainty depends crucially on having found the global solution of the model. This is made possible by the development of a novel deep learning method for solving recursive economic models under aggregate uncertainty.

Several factors not incorporated in this model are likely to further complicate the role of housing wealth in shaping inequalities in climate damages. Three such factors are belief heterogeneity, agglomeration, and growth. In reality, beliefs about climate change vary significantly across individuals. In a world with such belief heterogeneity, households who more accurately predict the consequences of climate change might be more likely to gain from forward-looking decisions informed by those beliefs. In reality, productivity is

shaped by agglomeration forces as well as exogenous geographic advantages. If these amplify the spatial reallocation of economic activity due to climate change, they may also amplify the impacts of climate change on housing prices. Economic and population growth are also significant factors shaping housing prices. Especially because climate change occurs on the scale of centuries, the interaction of growth with climate change may have the potential to dramatically shape house price and welfare impacts.

Finally, this model develops methods with potentially interesting applications beyond the climate literature. All housing wealth depends on housing prices which reflect uncertain expectations. In reality, expectations and uncertainty over many long-term developments shape housing prices in the present. Dynamic spatial models with heterogeneous households, homeownership, and aggregate uncertainty—together with the numerical methods advances introduced here—could be used to study the impacts of expectations regarding future zoning policy, population growth, or future agglomeration forces on housing markets.

References

- Albouy, D., Graf, W., Kellogg, R., & Wolff, H. (2016). Climate Amenities, Climate Change, and American Quality of Life [Publisher: The University of Chicago Press]. *Journal of the Association of Environmental and Resource Economists*, 3(1), 205–246. <https://doi.org/10.1086/684573>
- Azinovic, M., Gaegauf, L., & Scheidegger, S. (2022). Deep Equilibrium Nets [_eprint: <https://onlinelibrary.wiley.com/doi/pdf/10.1111/iere.12575>]
- Balboni, C. (2021). In Harm's Way? Infrastructure Investments and the Persistence of Coastal Cities.
- Bates, P. D., Quinn, N., Sampson, C., Smith, A., Wing, O., Sosa, J., Savage, J., Olcese, G., Neal, J., Schumann, G., Giustarini, L., Coxon, G., Porter, J. R., Amodeo, M. F., Chu, Z., Lewis-Gruss, S., Freeman, N. B., Houser, T., Delgado, M., ... Krajewski, W. F. (2021). Combined Modeling of US Fluvial, Pluvial, and Coastal Flood Hazard Under Current and Future Climates [_eprint: <https://onlinelibrary.wiley.com/doi/pdf/10.1029/2020WR028673>]. *Water Resources Research*, 57(2), e2020WR028673. <https://doi.org/10.1029/2020WR028673>
- Bilal, A., & Rossi-Hansberg, E. (2023). Anticipating Climate Change Across the United States. <https://doi.org/10.3386/w31323>
- Borusyak, K., Dix-Carneiro, R., & Kovak, B. (2022). Understanding Migration Responses to Local Shocks.
- Crews, L. (2023). A Dynamic Spatial Knowledge Economy.
- Deryugina, T., & Hsiang, S. (2017). *The Marginal Product of Climate* (tech. rep. w24072). National Bureau of Economic Research. Cambridge, MA. <https://doi.org/10.3386/w24072>
- Desmet, K., Kopp, R. E., Kulp, S. A., Nagy, D. K., Oppenheimer, M., Rossi-Hansberg, E., & Strauss, B. H. (2021). Evaluating the Economic Cost of Coastal Flooding. *American Economic Journal: Macroeconomics*, 13(2), 444–486. <https://doi.org/10.1257/mac.20180366>
- Favilukis, J., Ludvigson, S. C., & Van Nieuwerburgh, S. (2017). The Macroeconomic Effects of Housing Wealth, Housing Finance, and Limited Risk Sharing in General Equilibrium [Publisher: The University of Chicago Press]. *Journal of Political Economy*, 125(1), 140–223. <https://doi.org/10.1086/689606>
- Fernandez-Villaverde, J., Nuno, G., Sorg-Langhans, G., & Vogler, M. (2020). Solving High-Dimensional Dynamic Programming Problems using Deep Learning, 48.
- Fried, S. (2022). Seawalls and Stilts: A Quantitative Macro Study of Climate Adaptation. *The Review of Economic Studies*, 89(6), 3303–3344. <https://doi.org/10.1093/restud/rdab099>
- Giannone, E., Paixão, N., Pang, X., & Li, Q. (2023). A Quantitative Spatial Equilibrium Model with Wealth.
- Greaney, B. (2021). The Distributional Effects of Uneven Regional Growth, 49.

- Han, J., Yang, Y., & E, W. (2021). DeepHAM: A Global Solution Method for Heterogeneous Agent Models with Aggregate Shocks. *SSRN Electronic Journal*. <https://doi.org/10.2139/ssrn.3990409>
- Hsiang, S., Kopp, R., Jina, A., Rising, J., Delgado, M., Mohan, S., Rasmussen, D. J., Muir-Wood, R., Wilson, P., Oppenheimer, M., Larsen, K., & Houser, T. (2017). Estimating economic damage from climate change in the United States. *Science*, 356(6345), 1362–1369. <https://doi.org/10.1126/science.aal4369>
- Hsiao, A. (2023). Sea Level Rise and Urban Adaptation.
- Kaplan, G., Mitman, K., & Violante, G. L. (2020). The Housing Boom and Bust: Model Meets Evidence [Publisher: The University of Chicago Press]. *Journal of Political Economy*, 000–000. <https://doi.org/10.1086/708816>
- Kleinman, B., Liu, E., & Redding, S. J. (2023). Dynamic Spatial General Equilibrium, 46.
- Knutson, T., Camargo, S. J., Chan, J. C. L., Emanuel, K., Ho, C.-H., Kossin, J., Mohapatra, M., Satoh, M., Sugi, M., Walsh, K., & Wu, L. (2020). Tropical Cyclones and Climate Change Assessment: Part II: Projected Response to Anthropogenic Warming [Publisher: American Meteorological Society Section: Bulletin of the American Meteorological Society]. *Bulletin of the American Meteorological Society*, 101(3), E303–E322. <https://doi.org/10.1175/BAMS-D-18-0194.1>
- Komissarova, K. (2022). Location Choices over the Life Cycle: The Role of Relocation for Retirement.
- Krusell, P., & Smith, A. A., Jr. (1998). Income and Wealth Heterogeneity in the Macroeconomy. *Journal of Political Economy*, 106(5), 867–896. <https://doi.org/10.1086/250034>
- Krusell, P., & Smith, A. A., Jr. (2022). Climate Change Around the World.
- Maliar, L., Maliar, S., & Winant, P. (2021). Deep learning for solving dynamic economic models. *Journal of Monetary Economics*, 122, 76–101. <https://doi.org/10.1016/j.jmoneco.2021.07.004>
- Pang, X., & Sun, P. (2023). MOVING INTO RISKY FLOODPLAINS:
- Rasmussen, D., & Kopp, R. E. (2017). Probability-Weighted Ensembles Of U.S. County-Level Climate Projections For Climate Impact Modeling [Publisher: Zenodo]. <https://doi.org/10.5281/ZENODO.582327>
- Rode, A., Carleton, T., Delgado, M., Greenstone, M., Houser, T., Hsiang, S., Hultgren, A., Jina, A., Kopp, R. E., McCusker, K. E., Nath, I., Rising, J., & Yuan, J. (2021). Estimating a social cost of carbon for global energy consumption [Number: 7880 Publisher: Nature Publishing Group]. *Nature*, 598(7880), 308–314. <https://doi.org/10.1038/s41586-021-03883-8>
- Saiz, A. (2010). The Geographic Determinants of Housing Supply [Publisher: Oxford Academic]. *The Quarterly Journal of Economics*, 125(3), 1253–1296. <https://doi.org/10.1162/qjec.2010.125.3.1253>
- Sinai, T., & Souleles, N. S. (2005). Owner-Occupied Housing as a Hedge Against Rent Risk*. *The Quarterly Journal of Economics*, 120(2), 763–789. <https://doi.org/10.1093/qje/120.2.763>

Wing, O. E. J., Lehman, W., Bates, P. D., Sampson, C. C., Quinn, N., Smith, A. M., Neal, J. C., Porter, J. R., & Kousky, C. (2022). Inequitable patterns of US flood risk in the Anthropocene [Number: 2 Publisher: Nature Publishing Group]. *Nature Climate Change*, 12(2), 156–162. <https://doi.org/10.1038/s41558-021-01265-6>

Yao, R., & Zhang, H. H. (2005). Optimal Consumption and Portfolio Choices with Risky Housing and Borrowing Constraints. *Review of Financial Studies*, 18(1), 197–239. <https://doi.org/10.1093/rfs/hhh007>

A Harmonization of Climate Damage Estimates

A.1 Labor Productivity

I take estimates of the effect of temperature on wages from Deryugina and Hsiang, 2017. They use a panel of U.S. counties from 1969 to 2014 to estimate the effect of temperature on wages, using idiosyncratic weather variation. Although they do not study the effect of long-term adaptation, they argue that, in equilibrium, the marginal response of income to short-term weather realizations is equal to the marginal effect of income to long-term climate variation. They use an envelope-theorem argument: in the neighborhood of equilibrium temperatures, the benefit of long-term climate adaptations must be zero.

They thus estimate the effect of daily temperatures on log annual total income per capita. Their Figure 4a (my Figure 27) shows their estimates. They choose 55°F as the reference temperature, because it is the temperature with the greatest positive effect on productivity in their estimation. I recenter at 65°F. Upon recentering, the marginal effect of temperatures above 65°F remains fairly constant. The overall effect of temperatures below 65°F is negative but small, with an average effect of 6.6×10^{-6} per °C-day between 15°F and 65°F, an order of magnitude smaller than the average effect of -4.5×10^{-5} per °C-day between 65°F and 85°F. It is true, however, that the marginal effect of temperatures below 65°F is not constant, and it would be ideal to use projections of HDD and CDD centered at 55°F. Table 1 shows these extracted estimates.

Using climate projections on HDD and CDD changes per °C global warming, as in Section 3.3.2, I compute income damages for each county per °C global warming. Figure 2 displays the resulting projections of income reductions for each PUMA.

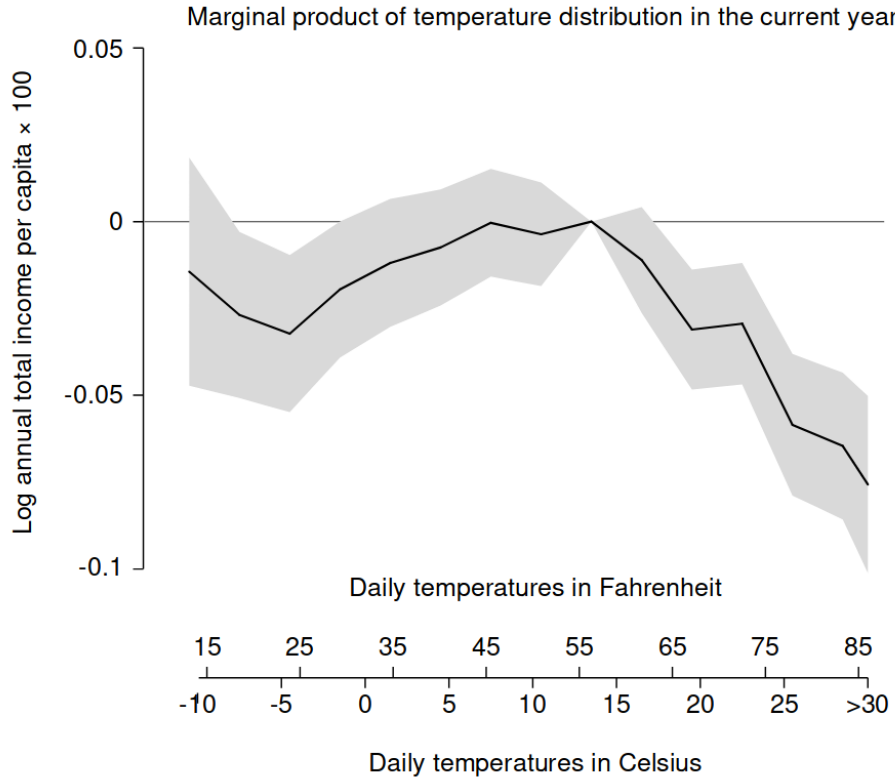


Figure 27: Impact of a single day at a certain temperature on log annual total income. Reproduced from Deryugina and Hsiang, 2017.

A.2 Disaster Projections

I use projections of climate impacts on total combined damages from flooding from Bates et al. (2021), as reported in Wing et al. (2022).

I argue that their projections, together with the estimates I use on heat and cold amenities, capture the great majority of climate impacts on natural disasters. Of the 18 FEMA hazard categories, “Earthquake” and “Volcano” are likely not climate-sensitive. “Wildfire,” “Heat Wave,” “Cold Wave,” “Winter Weather,” “Ice Storm,” “Drought,” “Avalanche,” and “Hail” are not separately identified from the estimates on heat and cold climate amenities which I take from the literature (Section 3.3.2). This leaves primarily flooding and wind-related hazards and wind-related hazards—“Coastal Flooding,” “Landslide,” “Riverine Flooding,” “Tsunami,” “Hurricane,” “Tornado,” “Strong Wind,” “Lightning.”

The projections I use are likely to capture the great majority of our current best understanding of the climate-sensitivities of flooding and wind-related disasters. These projections include all forms of flooding, including those which happen in conjunction with storms, leaving primarily wind-related damages. Current projections of the impact of climate change on wind-related damages *per se* are highly uncertain, with

confidence intervals centered near zero.

A recent meta-analysis of projections of tropical cyclone activity under climate change (Knutson et al., 2020), find confident projections of increasing tropical cyclone precipitation, but small and highly uncertain changes in terms of wind speeds. Among the models they survey, median projections for a 2° warming scenario predict a 16% *decrease* in tropical cyclone frequencies in the North Atlantic basin, but a 3% increase in average intensity. the net result is a 10% increase in the annual number of category 4-5 cyclones, with an interquartile range of [-21%, 28%]. Cyclone intensity refers to wind speed only, and this uncertainty does not extend to precipitation and flooding. The median projected increase in precipitation under the 2°C warming scenario is 16% with interquartile range [8%, 21%]. Flooding due to storm surges is also projected to increase, due to rising sea levels (Little et al. 2015). Indeed, the greatest impact of climate change on property damages are expected to take the form of these “compound events,” (AghaKouchak et al., 2020) and compound events which include flooding are encompassed by the projections I use.

As a test of this coverage, I compare the mean annual residential flooding damages, or Average Annual Losses (AAL), from all contiguous U.S. flooding, under 2020 climate conditions, predicted by the model of Bates et al. (2021). Their prediction is \$30bn, which actually exceeds the mean annual damages in SHELDUS between 2011 and 2020 in the “Coastal Flooding,” “Hurricane,” “Riverine Flooding,” “Severe Storm,” and “Tsunami” categories. These realized damages are \$21.39bn (2021 USD) and account for 71% of all realized property damage from disasters in that period.

Due to data limitations, I have only two variables per county from the analysis of Bates et al. (2021). The first is Average Annual Losses (AAL), per county, given 2020 climate conditions. The second is the percentage change in AAL per county between 2020 and 2050 under RCP 4.5. In order to harmonize this with the other estimates, I divide the AAL change by 0.63°C, the median global warming under RCP 4.5 in that time period (Rasmussen and Kopp, 2017). This gives me a linearized measure of the projected increase in AAL per °C global warming:

$$\frac{d}{dT} \widehat{\text{AAL}}_\ell(T) = \frac{\text{AAL}_{\ell,2050} - \text{AAL}_{\ell,2020}}{0.63 \text{ } ^\circ\text{C}}$$

A.3 Heat and Cold Amenities

I take estimates of heat and cold amenities from Albouy et al., 2016, who use a Rosen-Roback style model and the IPUMS 5% sample of the 2000 Census to impute amenities for each U.S. PUMA as the residual of real wage differentials. Thus, I am not double-counting the impact of temperatures on wages. They factor energy costs into real wages, so that I am not double-counting the impact of energy costs. They estimate a range of specifications.

I pick the richest model that is consistent with my model, reported in their Figure 5F (my Figure

28b). The dependent variable is willingness-to-pay (WTP) to avoid a single day at a certain temperature, and experience a day at 65°F instead. They fit WTP to a four-piece linear spline with geographic, non-temperature weather, and demographic controls, and state fixed effects. All other specifications use fewer controls, except for their Figure 5E (my Figure 28a), which fits WTP to a 7th-degree cubic spline.

The cubic spline specification is very close to linear for temperatures less than 65°F, and close to linear between 65°F and 85°F, but constant above 85°F, possibly due to lack of data. The linear specification separately estimates slopes below 45°F, between 45°F and 65°F, between 65°F and 80°F, and above 80°F. They find similar slopes for both segments below 65°F and both segments above 65°F. I therefore believe that it is not unreasonable to assume constant, but different, marginal effects for days below and above 65°F, respectively. I take their estimates for WTP at each extreme, 0°F and 110°F, and assume constant marginal value of each degree-day below and above 65°F.³²

Assuming constant marginal effects of each degree-day below and above 65°F allows me to impute cold disamenities as a function of annual heating-degree-days (HDD), the sum over each day t of the year

$$\sum_t \max(65^\circ\text{F} - T_t, 0)$$

of the number of degrees by which that day's temperature T_t falls below 65°F. I similarly impute heat disamenities as a function of annual 65°F-baseline cooling-degree-days (CDD). I report these WTP per degree-day estimates in Table 2.

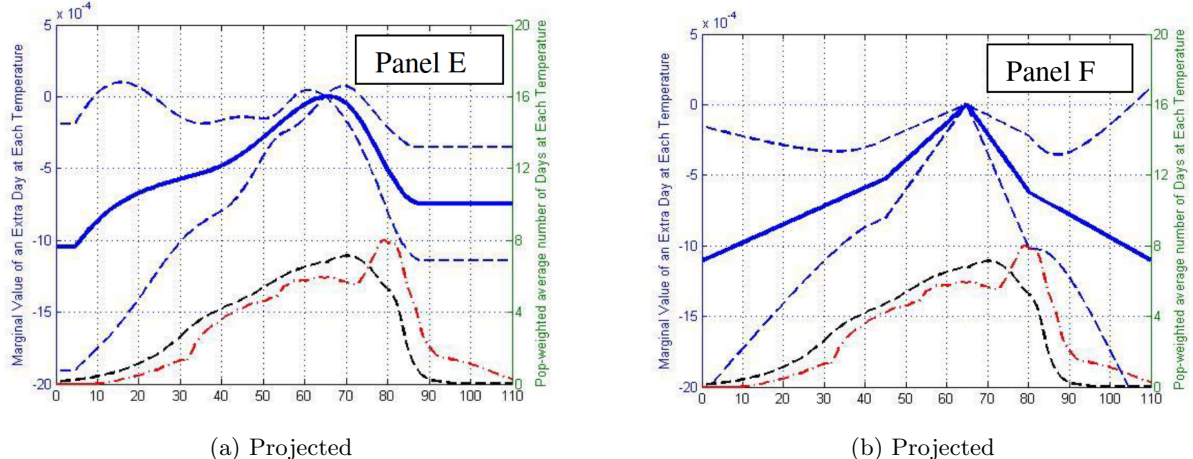


Figure 28: Marginal value of a day at a given temperature, relative to a day at 65°F, as a percentage of annual income. From: Albouy et al., 2016, Figure 9

³²Equivalently, I take the arithmetic mean of each pair of segments, weighted by segment length.

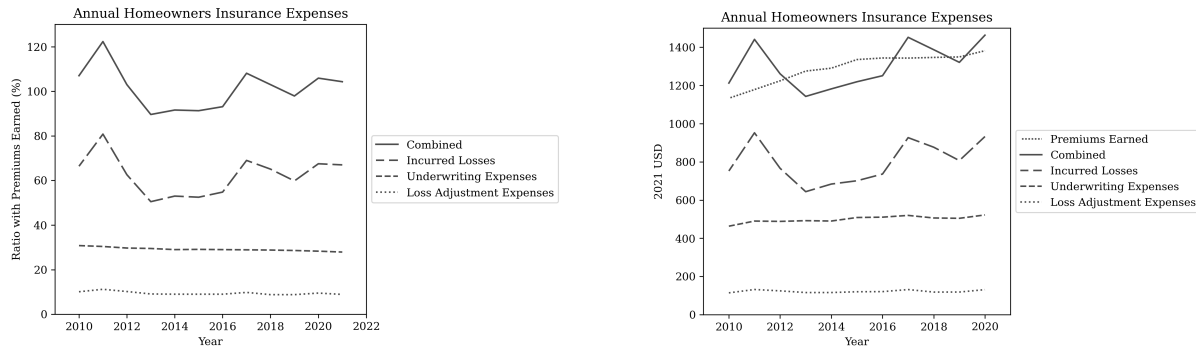
B State Space Model for Insurance Estimation

B.1 Data Sources

I use annual data for the U.S. between 2003 and 2020, compiled by the Insurance Information Institute (III), on average homeowners insurance premiums, average losses per policy-year, sources of losses, and sources of expenses. Expenses are divided first into incurred losses (i.e. payouts to policyholders), adjustment expenses, and underwriting and other expenses. Incurred losses are categorized by hazard (e.g. water damage, theft, etc.). These data are originally reported by the National Association of Insurance Commissioners and by Insurance Services Office, Inc. I use data on global annual greenhouse gas emissions from the World Resources Institute.

B.2 Estimating Anticipated Losses

Accounting variables such as insurance losses and expenses are reported as the ratio between that variable and total earned premiums. “Incurred losses” are total claims paid to policyholders for a year, and “loss adjustment expenses” are additional expenses related to investigating and settling claims. I group all other expenses into “underwriting expenses,” or expenses related to originating or maintaining insurance policies rather than handling claims.



(a) Breakdown of expenses experienced by insurers from homeowners insurance business (ratio with premiums earned%). The combined ratio is the sum of the loss ratio (incurred losses divided by premiums earned) and the expense ratio (expenses divided by premiums earned). When the combined ratio is greater than 100, the insurer is losing money. Data are from the Insurance Information Institute (III).

(b) Breakdown of expenses experienced by insurers from homeowners insurance business (2021 dollars). Data are the same as the left figure, but values are given in dollar terms instead of as a ratio with premiums earned.

Figure 29

Figures 29a and 29b show the breakdown of expenses experienced by homeowners insurance companies. The majority of expenses are incurred losses, with loss adjustment expenses and underwriting expenses each

accounting for about a quarter of total expenses.

The solid line indicates the “combined ratio,” a common metric used to assess the profitability of an insurance company. I assume that insurers are zero-profit, so that the anticipated combined ratio is equal to 100. I use this assumption to back out the expected level of incurred losses that insurers anticipate paying each year.³³

Figure 30 shows the average homeowners insurance premium and estimated anticipated losses, 2003-2020, in 2021 USD. The estimated anticipated losses appear to track the mean of realized losses well.

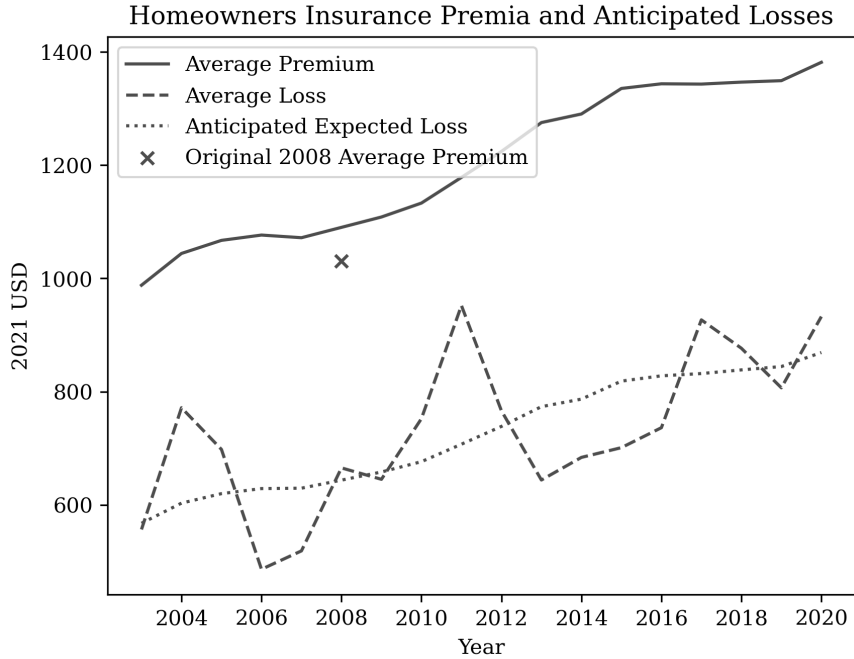


Figure 30: Average homeowners insurance premium and estimated anticipated losses, 2003-2020, in 2021 USD. The only significant decrease in average premium, in the original data, occurs in 2008, and is immediately reversed in 2009. I drop this observation on the grounds that it is likely a transient change due to the financial crisis rather than a persistent change in climate beliefs. Dollar losses (expenses) are imputed by multiplying the loss (expense) ratio by the average premium. Prior to 2010, dollar losses are imputed by multiplying claim frequencies (claims per 100 policy-years) by claim severity (average amount paid per claim). Nominal values are deflated by CPI.

B.2.1 Linear Regression

I show here that reduced-form evidence suggests that homeowners insurance premiums are responsive to disaster realizations in such a way that suggests that insurers are uncertain about the true distribution from which these realizations are drawn. I use this to inform a Bayesian estimation of the insurer’s uncertainty over the contribution of emissions to disaster risk in Appendix B.

³³Additional details of this imputation procedure are in Appendix C. Expenses consist of both fixed and variable expenses that depend on realized losses, which I must invert.

I begin by defining the simple estimating equation,

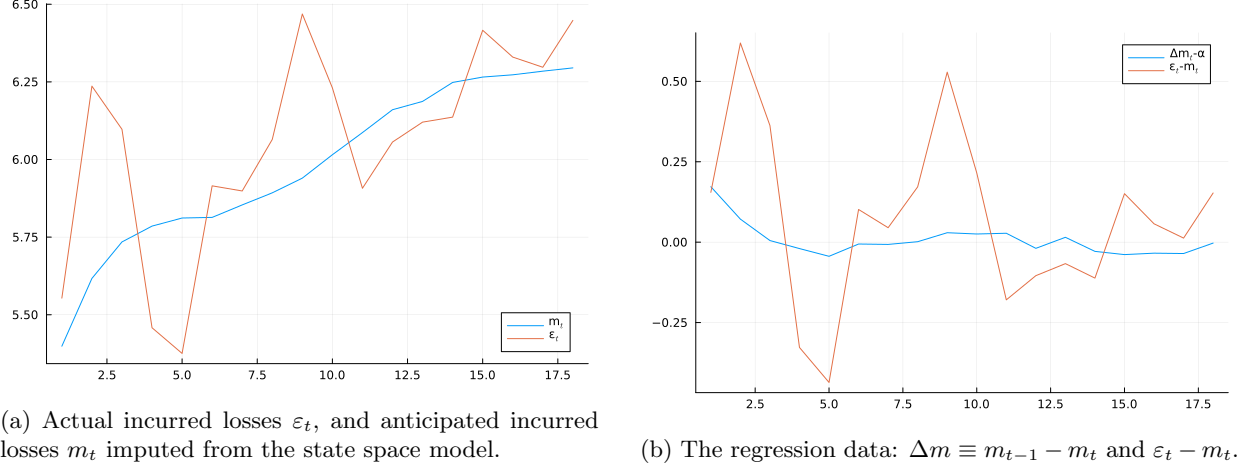
$$m_{t+1} - m_t = \alpha + \frac{\tilde{\sigma}^2}{\sigma_\varepsilon^2}(\varepsilon_t - m_t) + \frac{\tilde{\sigma}^2}{\sigma_\eta^2}(\eta_t - m_t). \quad (10)$$

where m_t is the insurer's prior mean of losses in year t , which I impute from the insurance premium (with details in Appendix C). ε_t is the insurer's realized losses in year t , and η_t is a news shock which explains residual variation in premiums.

That is, I simply regress changes in imputed prior means on observed (log) loss surprises ε_t , and use the model to interpret the reduced-form coefficient on ε_t . Although $m_t = L_t - (\sigma^2 + \sigma_\varepsilon^2)/2$ depends on parameters, the effect of these parameters is small, and can be solved for by fixed point. More seriously, unless $\mu_t = m_t$, the error term $\frac{\tau_\eta}{\tau}(\eta_t - m_t)$ will be biased and correlated with the regressor though the insurer's prior bias $\mu_t - m_t$,

$$\begin{aligned} \mathbb{E}[\eta_t - m_t] &= \mu_t - m_t \\ \text{Cov}(\varepsilon_t - m_t, \eta_t - m_t) &= (\mu_t - m_t)^2 - 2(\mu_t - m_t), \end{aligned}$$

so this should be considered a descriptive exercise. Figure 31b shows the data used in this regression.



(a) Actual incurred losses ε_t , and anticipated incurred losses m_t imputed from the state space model.

(b) The regression data: $\Delta m \equiv m_{t-1} - m_t$ and $\varepsilon_t - m_t$.

I estimate Equation 10 by OLS, and report the results in Table 8. In columns 5-8, I fix the intercept α at 0.77% to match the forecast of Wing et al. (2022) of a 26% increase in flooding damages over 30 years. In columns 1,2,5, and 6, I estimate the slightly modified Equation 11 in which the error is reduced-form and not modeled as a signal. In columns 2,4,6, and 8, I drop the first observation because it is by far the largest value of the regressor. In all specifications there is a significant effect of loss surprises on premiums, although the significance is lower when the first observation is included.

Table 8: Parameter estimates.

	(1)	(2)	(3)	(4)	(5)	(6)	(7)	(8)
α	0.046*** (0.012)	0.054*** (0.010)	0.046*** (0.012)	0.054*** (0.010)				
$\varepsilon - m_t$	0.083* (0.043)	0.076*** (0.022)	0.083* (0.043)	0.076*** (0.022)	0.166** (0.058)	0.095*** (0.024)	0.163** (0.059)	0.095*** (0.025)
N	18	17	18	17	18	17	18	17
R^2	0.190	0.453	0.190	0.453	0.326	0.485	0.313	0.483

$$m_{t+1} - m_t = \alpha + \frac{1}{1 + \sigma_\varepsilon^2 / \sigma^2} (\varepsilon_t - m_t) + \zeta_t. \quad (11)$$

B.3 Model

I attribute to a representative home insurer the same climate model as in the main model. Insurer storm losses $\exp(d_t)$ are generated by a persistent-transitory process. Log-losses d_t are drawn from a Normal distribution with unobserved mean μ_t , which follows a Gaussian random walk that is affected by emissions e_t . Each year, the insurer also observes a news shock n_t , unobserved to the econometrician, whose mean is a linear function of μ_t . Without loss of generality, η_t has mean μ_t . Formally,

$$\begin{aligned} \mu_{t+1} &= \rho\mu_t + \beta e_t \\ n_t &\sim \mathcal{N}(\mu_t, \sigma_n^2) \\ d_t &\sim \mathcal{N}(\mu_t, \sigma_d^2) \end{aligned}$$

The parameters $\{\sigma_n^2, \sigma_d^2, \rho\}$ are known to the insurer. The values $\{n_t, d_t, e_t\}$ are observed each period. The parameters β and μ_t are unobserved and learned about over time.

The timing of the model is as follows. Each period:

1. The insurer sets a premium π_t .
2. The shocks n_t and d_t are realized and observed.
3. The insurer updates their prior over μ_t and β .
4. The true mean μ_t is updated according to the AR(1) process.

If the insurer has an initial multivariate normal prior over μ_0 and β , then, if fully rational Bayesian learners, they update their beliefs according to the Kalman filter. Rewriting the model in terms of matrices:

$$\begin{aligned}\underbrace{\begin{bmatrix} d_t \\ n_t \end{bmatrix}}_{\mathbf{z}_t} &= \underbrace{\begin{bmatrix} 1 & 0 \\ 1 & 0 \end{bmatrix}}_{\mathbf{H}_t} \underbrace{\begin{bmatrix} \mu_t \\ \beta \end{bmatrix}}_{\mathbf{x}_t} + \mathbf{v}_t, \quad \mathbf{v}_t \sim \mathcal{N}(0, \Sigma_v) \\ \underbrace{\begin{bmatrix} \mu_{t+1} \\ \beta \end{bmatrix}}_{\mathbf{x}_{t+1}} &= \underbrace{\begin{bmatrix} \rho & e_t \\ 0 & 1 \end{bmatrix}}_{\mathbf{F}_t} \underbrace{\begin{bmatrix} \mu_t \\ \beta \end{bmatrix}}_{\mathbf{x}_t}\end{aligned}$$

If the insurer's prior for \mathbf{x}_t at the end of period $t - 1$ is

$$\mathbf{x}_t | \mathcal{I}_t \sim \mathcal{N} \left(\hat{\mathbf{x}}_t \equiv \begin{bmatrix} \hat{\mu}_t \\ \hat{\beta}_t \end{bmatrix}, \hat{\mathbf{P}}_t \right),$$

then their prior for \mathbf{x}_{t+1} at the end of period t is

$$\begin{aligned}\hat{\mathbf{x}}_{t+1} &= \mathbf{F}_t(\mathbf{I} - \mathbf{K}_t \mathbf{H}_t) \hat{\mathbf{x}}_t + \mathbf{F}_t \mathbf{K}_t \mathbf{z}_t \\ \hat{\mathbf{P}}_{t+1} &= \mathbf{F}_t(\mathbf{I} - \mathbf{K}_t \mathbf{H}_t) \hat{\mathbf{P}}_t \mathbf{F}_t' \\ \mathbf{K}_t &= \hat{\mathbf{P}}_t \mathbf{H}_t' (\mathbf{H}_t \hat{\mathbf{P}}_t \mathbf{H}_t' + \Sigma_v)^{-1}\end{aligned}$$

where \mathbf{K}_t is the optimal Kalman gain.

B.3.1 Nesting Step

I observe $\{d_t, e_t, \hat{x}_t\}$ and wish to estimate $\{\sigma_n, \sigma_d, \rho, \hat{\beta}_0\}$. First, I simply rewrite the above equations in terms of block matrices:

$$\begin{aligned} \begin{bmatrix} \mathbf{x}_{t+1} \\ \mathbf{z}_{t+1} \\ \hat{\mathbf{x}}_{t+1} \end{bmatrix} &= \begin{bmatrix} \mathbf{F}_{t+1} & 0 & 0 \\ \mathbf{H}_{t+1} & 0 & 0 \\ 0 & \mathbf{F}_t \mathbf{K}_t & \mathbf{F}_t (\mathbf{I} - \mathbf{K}_t \mathbf{H}_t) \end{bmatrix} \begin{bmatrix} \mathbf{x}_t \\ \mathbf{z}_t \\ \hat{\mathbf{x}}_t \end{bmatrix} + \begin{bmatrix} 0 \\ \mathbf{v}_t \\ 0 \end{bmatrix} \\ \begin{bmatrix} 0 \\ \mathbf{v}_t \\ 0 \end{bmatrix} &\sim \mathcal{N} \left(0, \begin{bmatrix} 0 & 0 & 0 \\ 0 & \mathbf{R}_t & 0 \\ 0 & 0 & 0 \end{bmatrix} \right) \\ \begin{bmatrix} d_t \\ \hat{\mu}_t \end{bmatrix} &= \begin{bmatrix} 0 & 0 & 0 & 1 & 0 & 0 \\ 0 & 0 & 0 & 0 & 1 & 0 \end{bmatrix} \begin{bmatrix} \mathbf{x}_{t+1} \\ \mathbf{z}_{t+1} \\ \hat{\mathbf{x}}_{t+1} \end{bmatrix} = \begin{bmatrix} 0 & 0 & 0 & 1 & 0 & 0 \\ 0 & 0 & 0 & 0 & 1 & 0 \end{bmatrix} \begin{bmatrix} \mu_t \\ \beta \\ n_t \\ d_t \\ \hat{\mu}_t \\ \hat{\beta}_t \end{bmatrix} \end{aligned}$$

Observe that, for any guess of the parameters $\{\sigma_n, \sigma_d, \rho, \hat{\beta}_0\}$, all of the matrices in this system are known to us. That is, we can treat the above as a linear Gaussian state space model and apply the Kalman filter to it. This is the nesting step.

B.3.2 State Space Model Estimation

For any prior and given set of parameters, the Kalman filter yields a likelihood of the observed data, in our case $\{d_t, \hat{\mu}_t\}$. I thus estimate the parameters by maximum likelihood. Table 9 displays the result.

After estimating parameters, the Kalman smoother provides estimates of the unobserved state. Figure 32 shows the results. Given the parameter estimates, variation in $\hat{\mu}_t$ is almost entirely due to variation in beliefs $\hat{\beta}_t$ about β , as opposed to being driven by beliefs that the unobserved mean μ_t has changed over time.

Variable	Estimate
σ_n^{err}	0.21306
σ_d^{err}	0.28874
ρ	0.98
T_0	1965.87

Table 9: Results of state space estimation. Point estimates are by maximum likelihood.

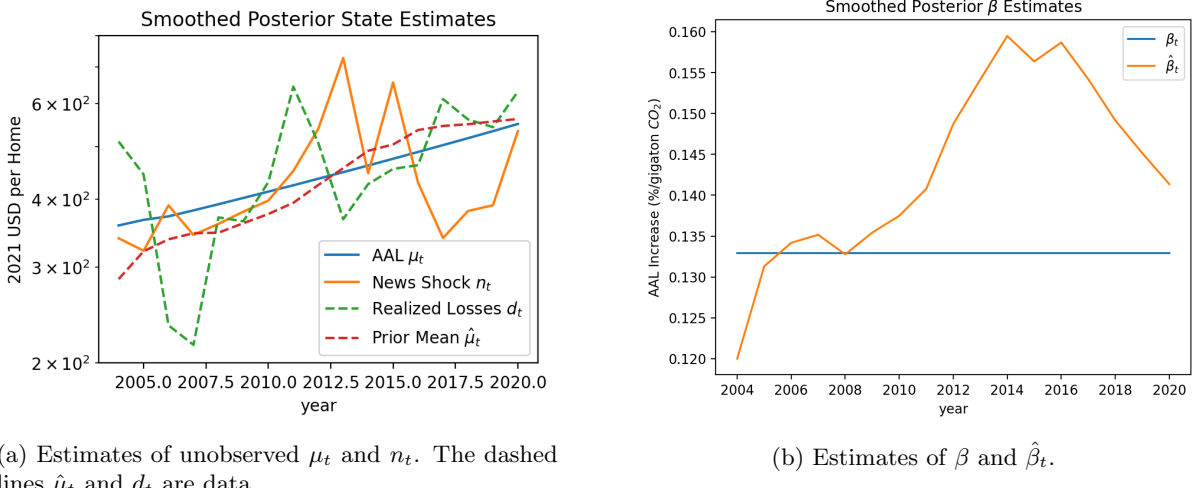


Figure 32

C Homeowners Insurance Anticipated Incurred Losses

In order to account for the fact that expenses other than the incurred expenses (henceforth “non-incurred expenses”) have a time trend and covary with incurred expenses, I regress non-incurred expenses on incurred losses and a time trend. That is, I decompose it into fixed and variable costs, where I allow for a time trend in fixed costs. Though the number of observations is small, the fit is very good. I regress non-incurred expenses on incurred losses and a time trend, and find a small time trend and . That is, I decompose it into fixed and variable costs, where I allow for a time trend in fixed costs.

$$\text{Expenses}_t = \alpha + \beta(\text{Incurred Losses})_t + \gamma\text{Year}_t + \varepsilon_t$$

Table 10: Expenses on incurred losses.

	Expense Ratio
Intercept	731.743*** (42.405)
Incurred Loss Ratio	0.079*** (0.009)
Year	-0.346*** (0.021)
R-squared	0.976
R-squared Adj.	0.970
N	12

I then assume risk-neutrality of insurers and apply the zero-profit condition that insurers are targeting a constant combined ratio of 100. I can thus estimate anticipated expected annual losses by setting anticipated expected combined losses equal premiums earned. By “anticipated expected” (henceforth simply “anticipated”) losses, I mean

$$\mathbb{E} [\text{Losses} \mid \mathcal{I}_t],$$

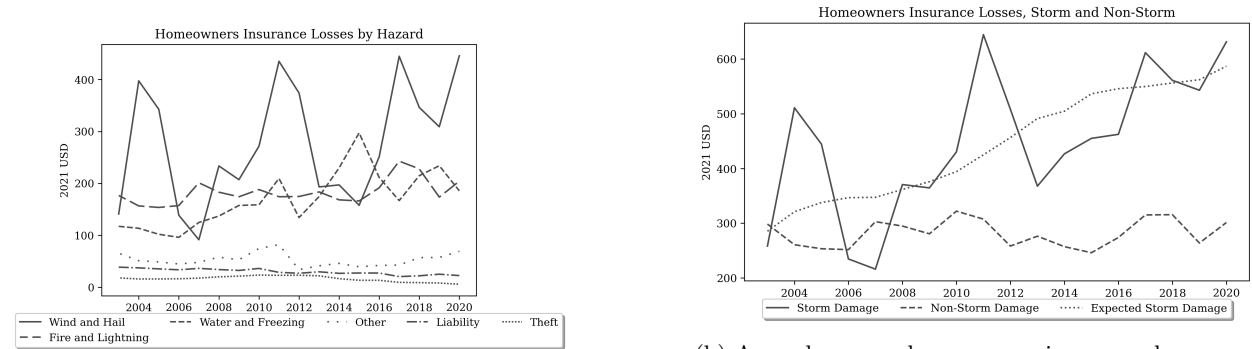
the expected value of anticipated losses given the insurer’s information set at time t . The mean combined ratio over the sample period was 101.425, suggesting that it is reasonable to assume that a value of 100 is targeted. Note that we would expect the combined ratio to be greater than 100 if insurers experience greater-than-expected losses over the sample period.

Let $\mathbb{E}[x \mid \mathcal{I}_t]$ denote the anticipated value of x conditional on the insurer’s information set at time t . For each year t , let L_t denote realized incurred loss ratio, N_t denote non-incurred expense ratio, and C_t denote the combined ratio. Then,

$$\begin{aligned}\mathbb{E}[C_t \mid \mathcal{I}] &= 100 \\ &= \mathbb{E}[L_t \mid \mathcal{I}] + \mathbb{E}[N_t \mid \mathcal{I}] \\ &= \mathbb{E}[L_t \mid \mathcal{I}] + \alpha + \beta \mathbb{E}[L_t \mid \mathcal{I}] + \gamma \text{Year}_t \\ \mathbb{E}[L_t \mid \mathcal{I}] &= (\mathbb{E}[C_t \mid \mathcal{I}] - \alpha - \gamma \text{Year}_t) / (1 + \beta)\end{aligned}$$

C.1 Storm Component of Losses

Figure 33a shows the breakdown of losses by hazard. Note that there is no clear trend in any category except “Wind and Hail” and “Water and Freezing.” In Figure, I group “Wind and Hail” and “Water and Freezing” losses into “Storm Losses” and all other incurred losses into “Non-Storm Losses.” The time trend of non-storm losses is vanishingly small, \$0.72/year. I thus assume that the time trend in anticipated non-storm losses is zero, and that all variation in anticipated losses is due to variation in anticipated storm losses. For each year, I simply subtract the sample mean of non-storm losses from total anticipated incurred losses to obtain my estimate of anticipated storm losses.



(a) Annual average homeowners insurance losses per policy-year, by hazard. Losses are reported in data as shares of total incurred losses, and are here imputed by multiplying by imputed total incurred losses.

(b) Annual average homeowners insurance losses per policy-year, by storm category. Losses are reported in data as shares of total incurred losses, and are here imputed by multiplying by imputed total incurred losses.

D Extreme-Value Location Preference Shocks

Integrating over the location preference shocks $\{\varepsilon_l'\}_l$ gives

$$\mathbb{E}V_{t+1}(b', z', h^{\text{live}'}, h^{\text{let}'}, \ell, a + 1) = \psi^{-1} \log \left(\sum_{\ell} \exp \left(\psi \tilde{V}_{\ell}(b, z, h_0^{\text{live}}, h_0^{\text{let}}, \ell_0, a) \right) \right)$$

where

$$\tilde{V}_{\ell}(b, z, h_0^{\text{live}}, h_0^{\text{let}}, \ell_0, a) = \max_{h^{\text{live}}, h^{\text{let}}, g, h} \tau d(\ell, \ell_0) + u(g, h, \alpha_{\ell t}) + \beta \mathbb{E}V_{t+1}(b', z', h^{\text{live}'}, h^{\text{let}'}, \ell, a + 1, \{\varepsilon_l'\}_l).$$

E Imputation Procedures